3.3.1.4. Day-30 Low-Flow Fiberglass Samples

A similar amount and composition of the film deposits were found with Day-30 low-flow fiberglass samples compared to Day-5 and Day-15 low-flow fiberglass samples. No significant difference was found regarding the amount of the film deposits between the exterior and the interior Day-30 low-flow fiberglass samples. As with the Day-5 and 15 samples, the film was composed of O, Na, Ca, Mg, Al, C, K, and possibly Si. Besides the film, a coating was found on the glass fibers (see Figure 3-39). The coating was likely formed by chemical precipitation. EDS analysis shows the coating had the same composition as the film, suggesting both are likely of chemical origin. Figures 3-37 through 3-43 show the Day-30 low-flow fiberglass results.

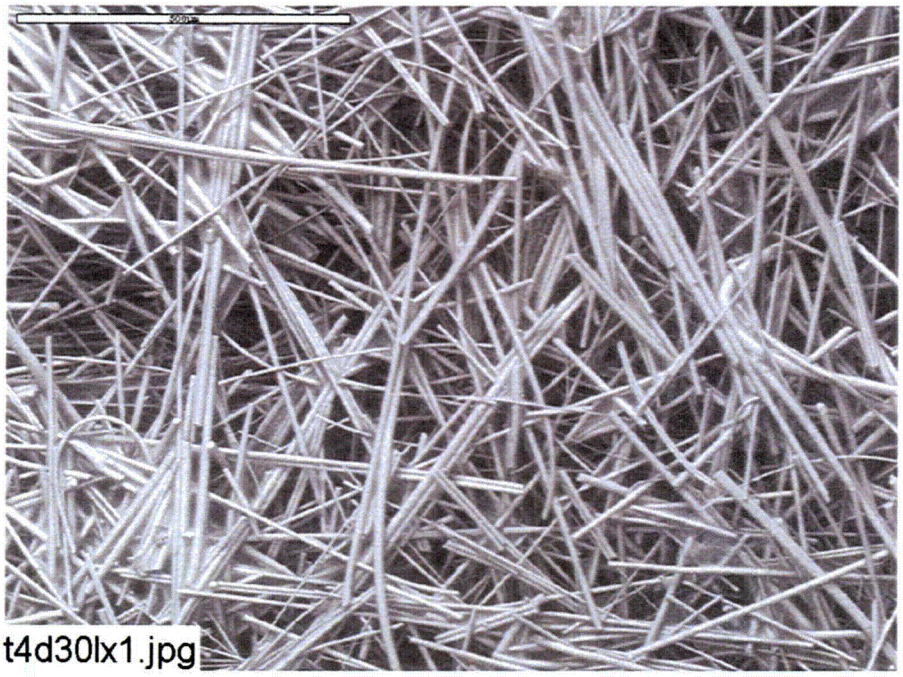

Figure 3-37. ESEM image magnified 100 times for a Test #4, Day-30 exterior low-flow fiberglass sample. (t4d30lx1.jpg)

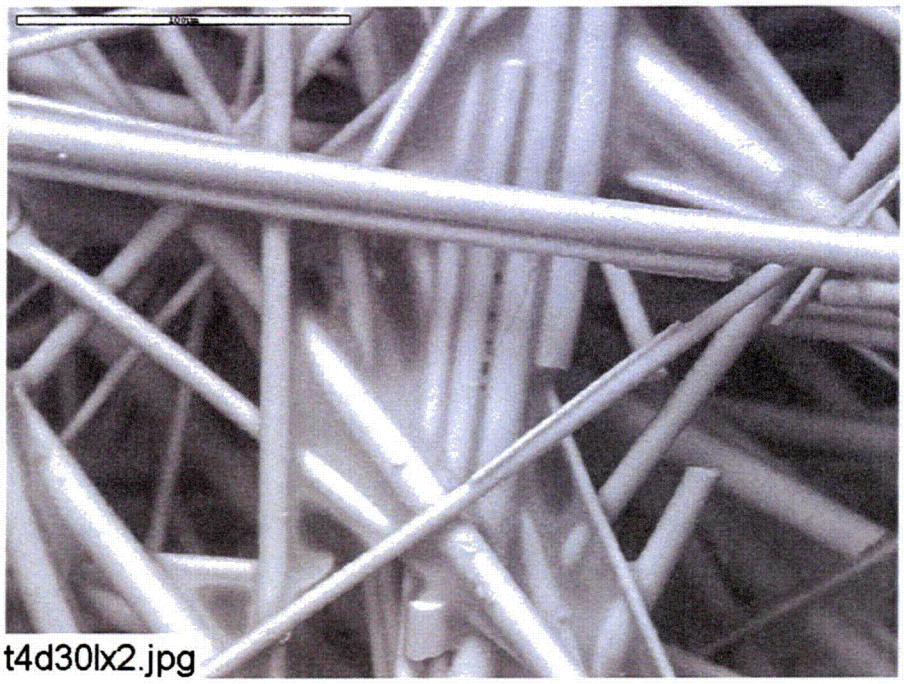

Figure 3-38. ESEM image magnified 500 times for a Test #4, Day-30 exterior low-flow fiberglass sample. (t4d30lx2.jpg)

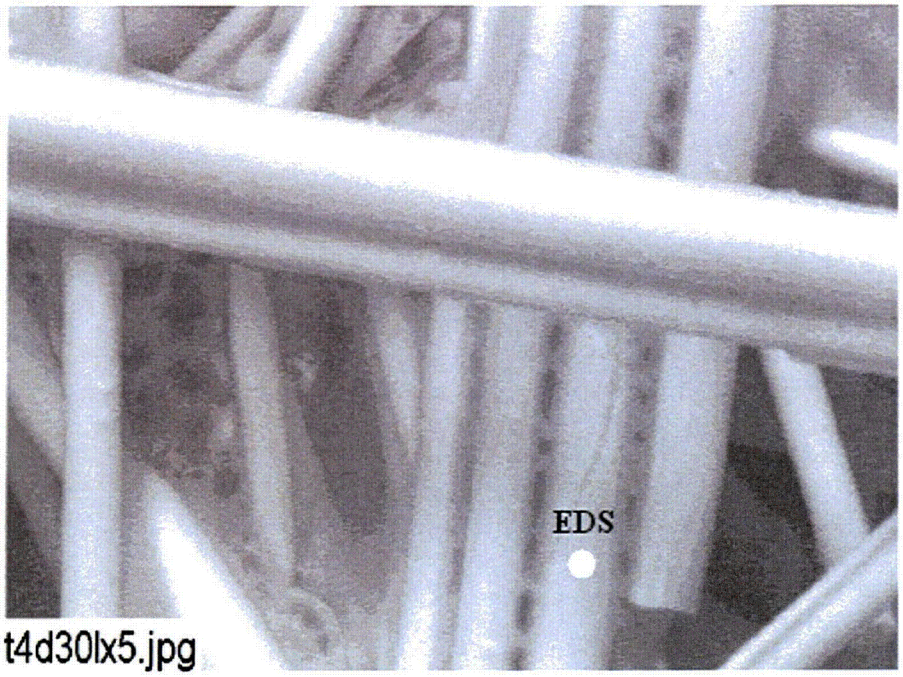

Figure 3-39. ESEM image magnified 1000 times for a Test #4, Day-30 low-flow fiberglass sample. (t4d30lx5.jpg)

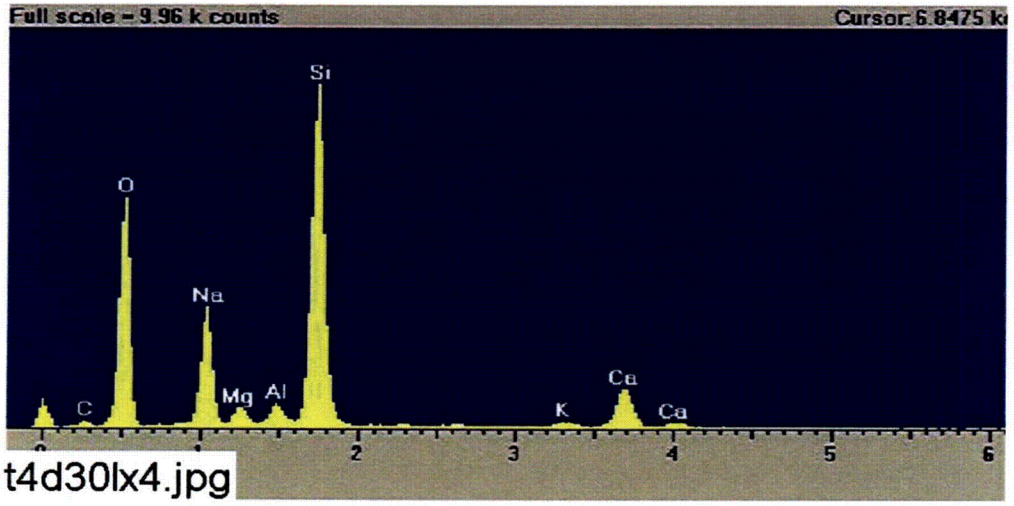

Figure 3-40. EDS counting spectrum for the spot of coating substance on the fiberglass shown in Figure 3-39. (t4d30lx4.jpg)

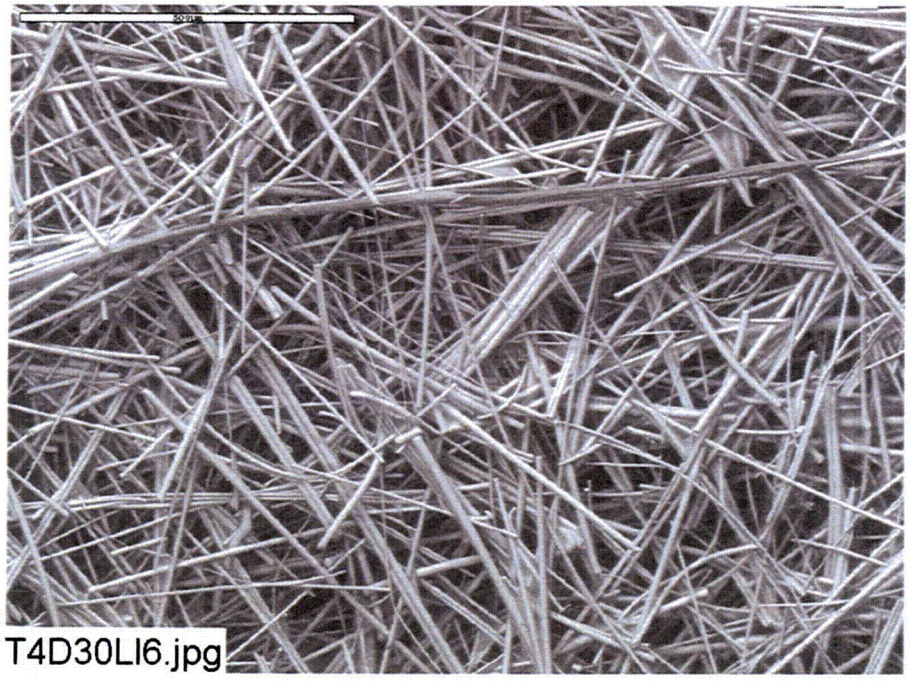

Figure 3-41. ESEM image magnified 100 times for a Test #4, Day-30 interior low-flow fiberglass sample. (T4D30LI6.jpg)

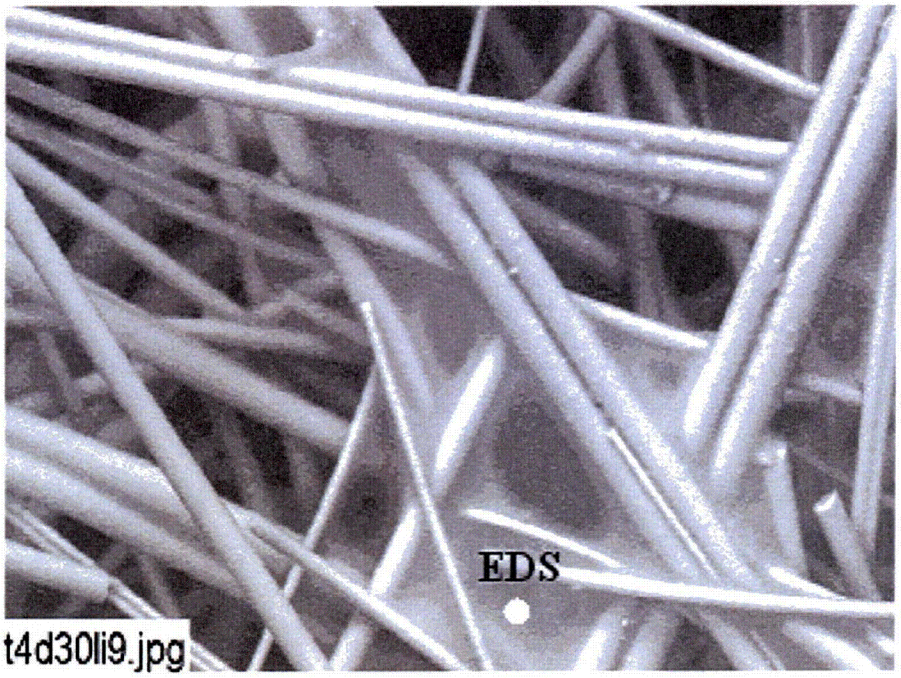

Figure 3-42. ESEM image magnified 500 times for a Test #4, Day-30 interior low-flow fiberglass sample. (t4d30li9.jpg)

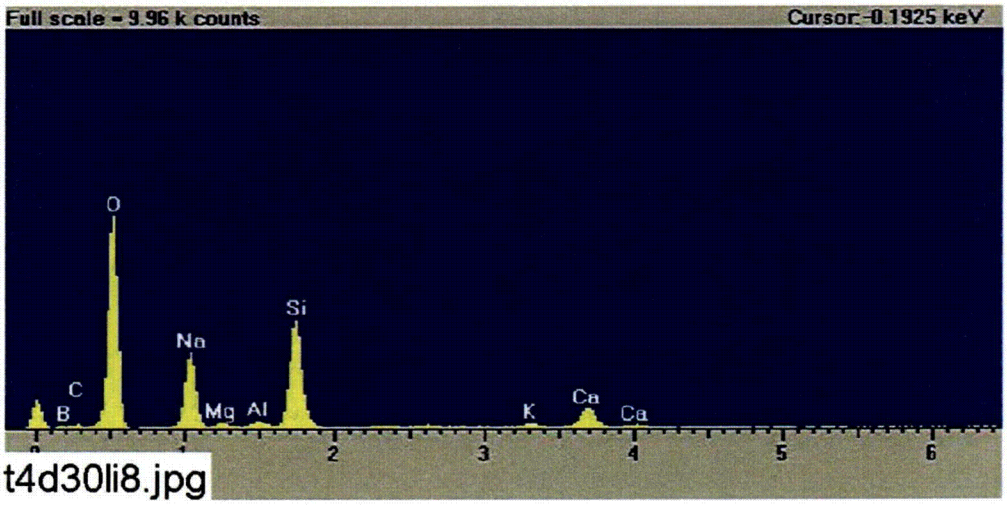

Figure 3-43. EDS counting spectrum for the film on the fiberglass shown in Figure 3-42. (t4d30li8.jpg)

3.3.1.5. Day-30 Fiberglass Inserted in Nylon Mesh in Low-Flow Zone

A 5 g fiberglass sample was enclosed in a nylon mesh and submerged in a low-flow zone of the tank on Day 3, to provide a comparison to all other fiberglass samples, which were enclosed in stainless steel mesh and placed in the tank on Day 0. The purpose of using a nylon mesh was to see if the mesh material (i.e., stainless steel or nylon) affects the deposits on the fiberglass samples. Comparing these results to Day-30 low-flow fiberglass samples, no significant difference was observed. The film was still the dominant deposit on both of the exterior and the interior samples. There were no particulate deposits found on the fiberglass. This result suggests that the mesh material did not significantly affect the deposits on fiberglass. In addition, ESEM images show that the nylon fiber was relatively clean and without significant deposits on it. The nylon mesh sample was put in the tank on Day 3, and no significant difference was found compared to the low-flow fiberglass samples put in the tank at the start of the test. Figures 3-44 through 3-49 show the Day-30 nylon-enclosed fiberglass results.

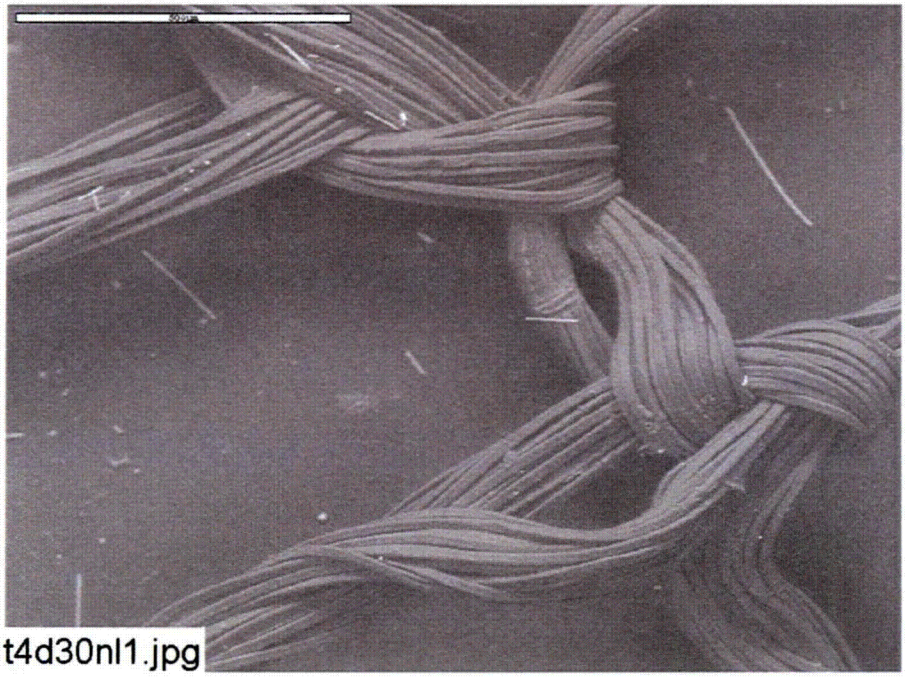

Figure 3-44. ESEM image magnified 100 times for a Test #4, Day-30 nylon mesh submerged in low-flow area (inserted on Day 4). (t4d30nl1.jpg)

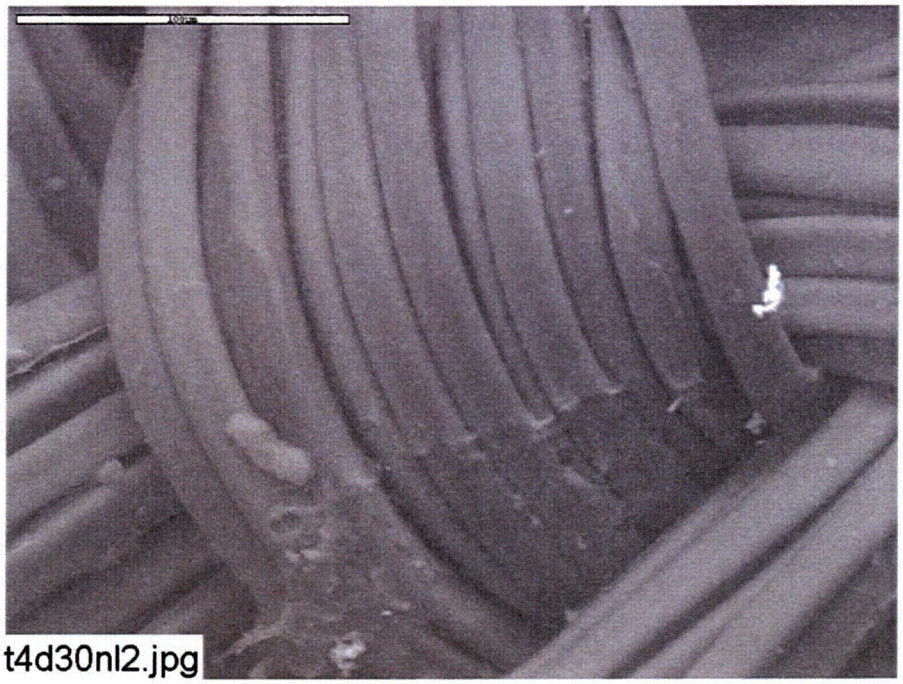

Figure 3-45. ESEM image magnified 500 times for a Test #4, Day-30 nylon mesh submerged in low-flow area (inserted on Day 4). (t4d30nl2.jpg)

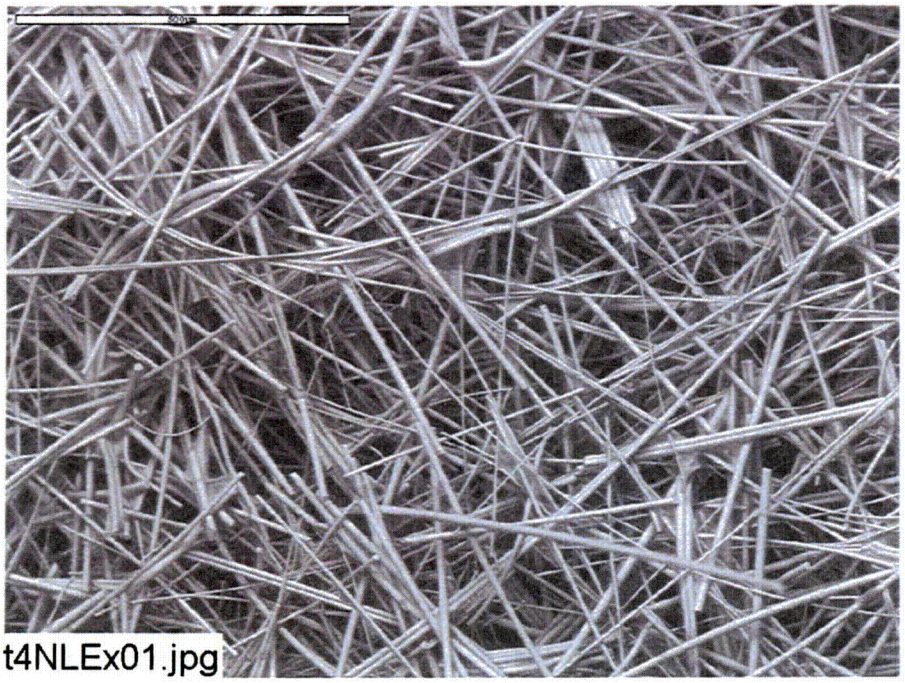

Figure 3-46. ESEM image magnified 100 times for a Test #4, Day-30 exterior low-flow fiberglass sample contained in a nylon mesh (inserted on Day 4). (t4NLEx01.jpg)

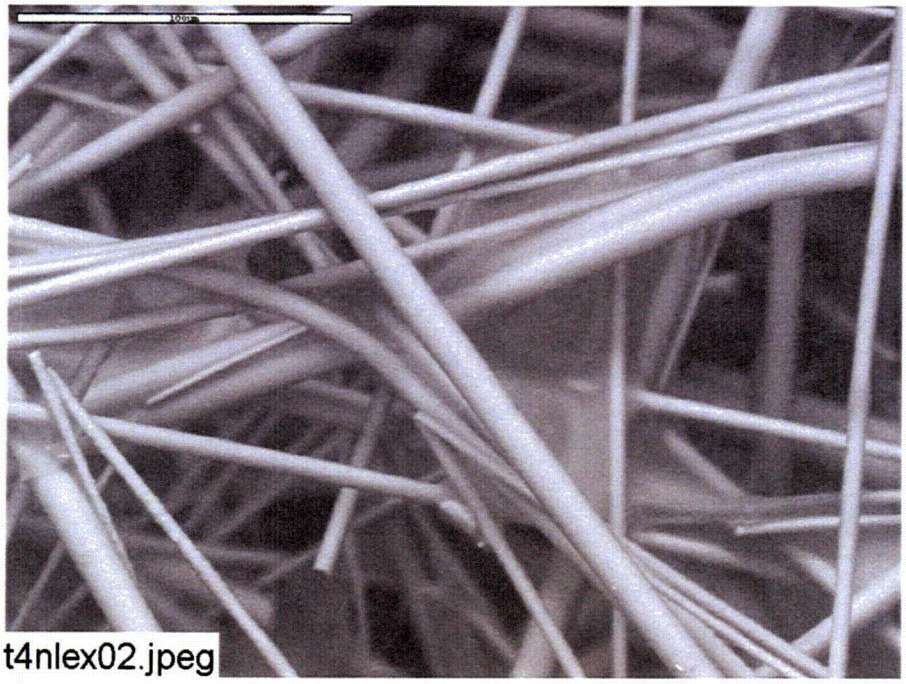

Figure 3-47. ESEM image magnified 500 times for a Test #4, Day-30 exterior low-flow fiberglass sample contained in a nylon mesh (inserted on Day 4). (t4nlex02.jpg)

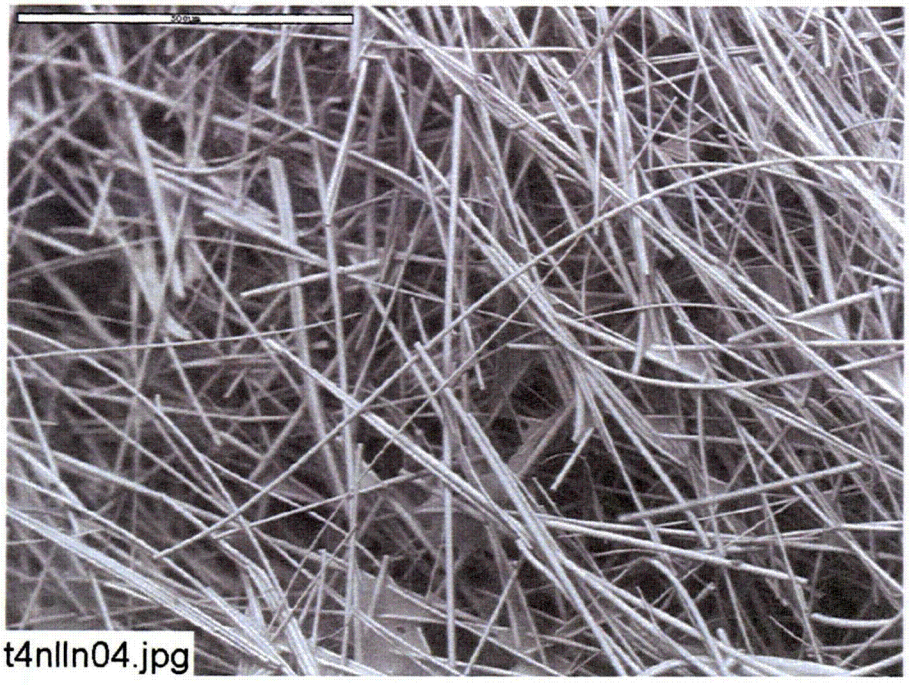

Figure 3-48. ESEM image magnified 100 times for a Test #4, Day-30 interior low-flow fiberglass sample contained in a nylon mesh (inserted on Day 4). (t4nlIn04.jpg)

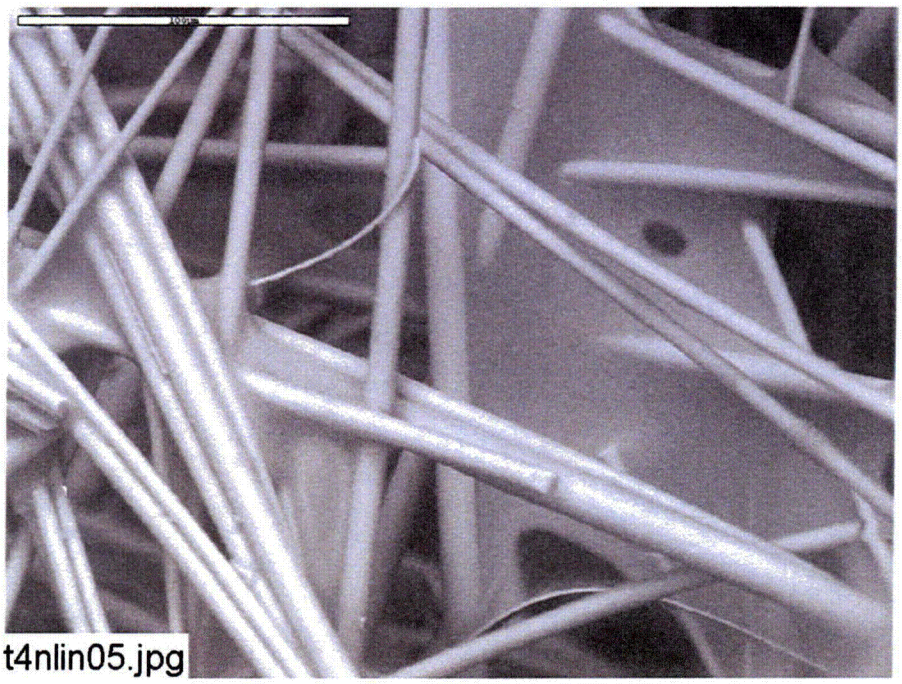

Figure 3-49. ESEM image magnified 500 times for a Test #4, Day-30 interior low-flow fiberglass sample contained in a nylon mesh (inserted on Day 4). (t4nlin05.jpg)

3.3.1.6. Day-30 Low-Flow Fiberglass Samples in the Big Envelope

Compared to other Day-30 low-flow fiberglass samples, a significant amount of particulate deposits was observed on the exterior of the Day-30 low-flow samples in the big envelope. The big envelope sat on the tank bottom and was in contact with the test sediment on the bottom of the envelope. Figure 3-120 shows the sediment after the samples were lifted out of the tank. However, no particulate deposits were observed on the fiberglass interior. In addition, some large flat fibers were found on the exterior fiberglass samples (see Figure 3-51). These large flat fibers were likely from cal-sil (see Appendix D). It is possible that the particulate deposits and cal-sil fibers were physically attached/retained on the exterior of the fiberglass samples. Figures 3-50 through 3-53 show the results from the Day-30 low-flow fiberglass enclosed in the big envelope. In contrast to other samples, these samples were gently rinsed with RO water and no film was found on either the exterior or the interior of the fiberglass. The disappearance of the film is likely caused by the rinse of RO water to keep the sample moist before ESEM analysis. Based on the control experiment noted earlier (see Appendix C4), the film is soluble.

Figure 3-50. ESEM image magnified 100 times for a Test #4, Day-30 exterior low-flow fiberglass sample in a big envelope. (t4evlx3.jpg)

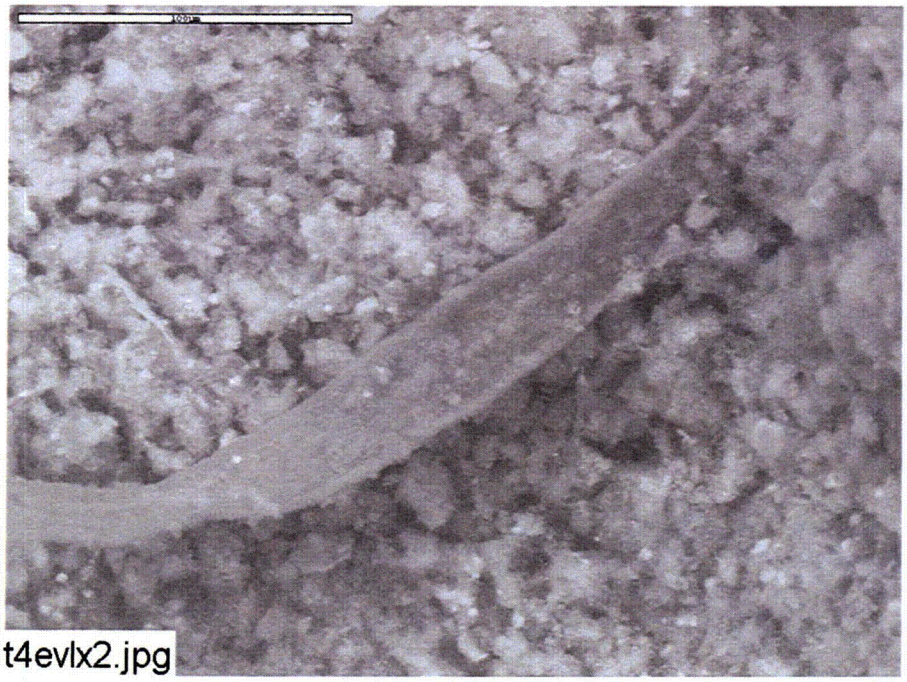

Figure 3-51. ESEM image magnified 500 times for a Test #4, Day-30 exterior low-flow fiberglass sample in a big envelope. (t4evlx2.jpg)

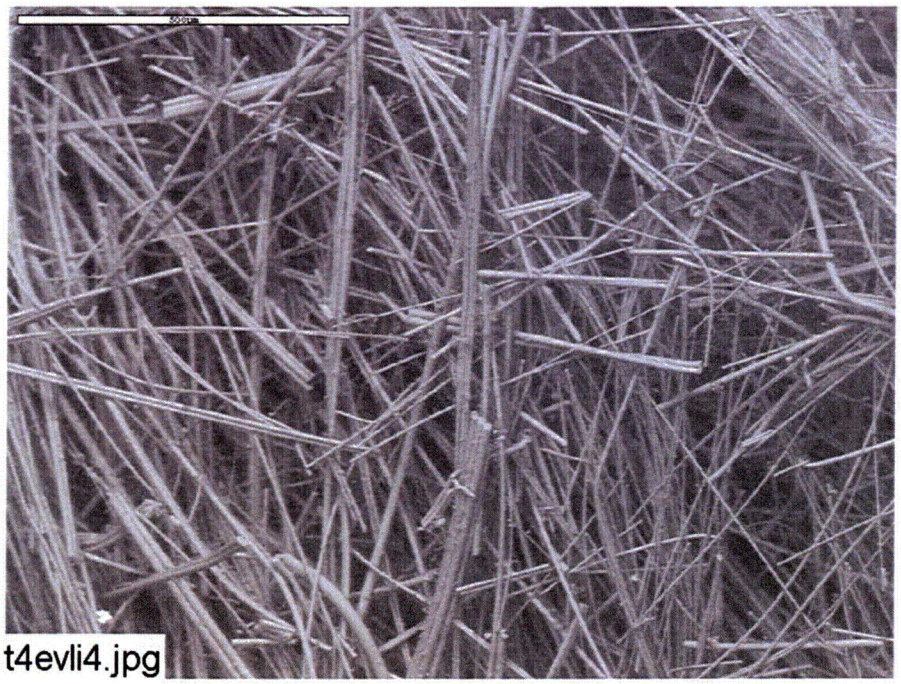

Figure 3-52. ESEM image magnified 100 times for a Test #4, Day-30 interior low-flow fiberglass sample in a big envelope. (t4evli4.jpg)

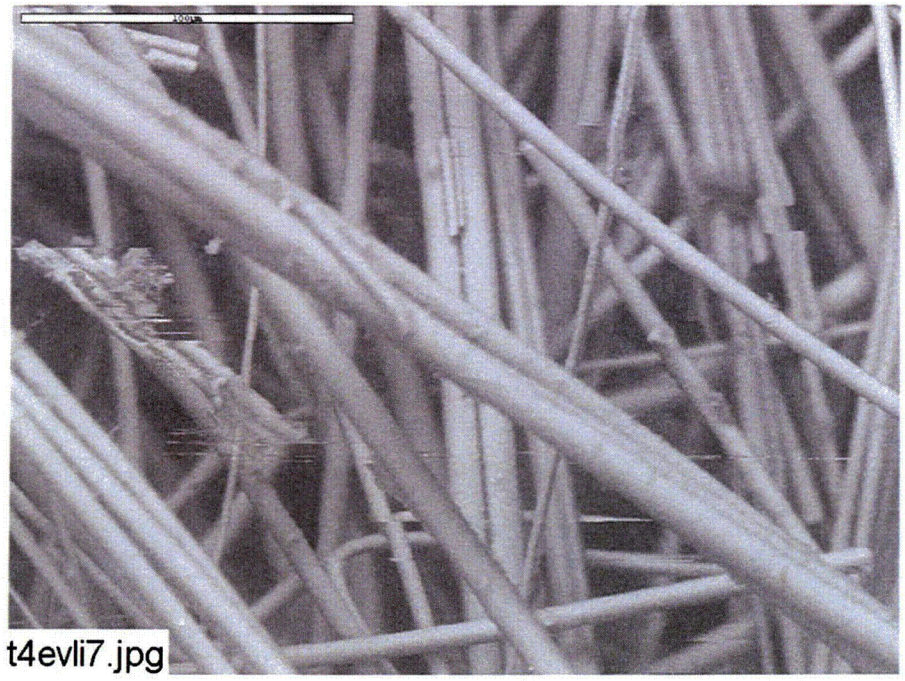

Figure 3-53. ESEM image magnified 500 times for a Test #4, Day-30 interior low-flow fiberglass sample in a big envelope. (t4evli7.jpg)

3.3.1.7. Day-30 High-Flow Fiberglass Samples

Compared to Day-30 low-flow fiberglass samples, a significant amount of particulate deposits and fiberglass debris were found on high-flow exterior samples. However, no particulate deposits were found on the interior. This result suggests that these particulate deposits were physically attached/retained on the fiberglass exterior. However, similar film deposits were found on both of the fiberglass exterior and the interior. The EDS result shows the film was composed of O, Na, Ca, C, Mg, Al, K, and possibly Si, which is similar to other EDS results. Figures 3-54 through 3-61 show the Day-30 high-flow fiberglass results. Figures 3-60 and 3-61 show fiberglass after it was rinsed with RO water.

Figure 3-54. ESEM image magnified 100 times for a Test #4, Day-30 exterior high-flow fiberglass sample. (T4HFEx01.jpg)

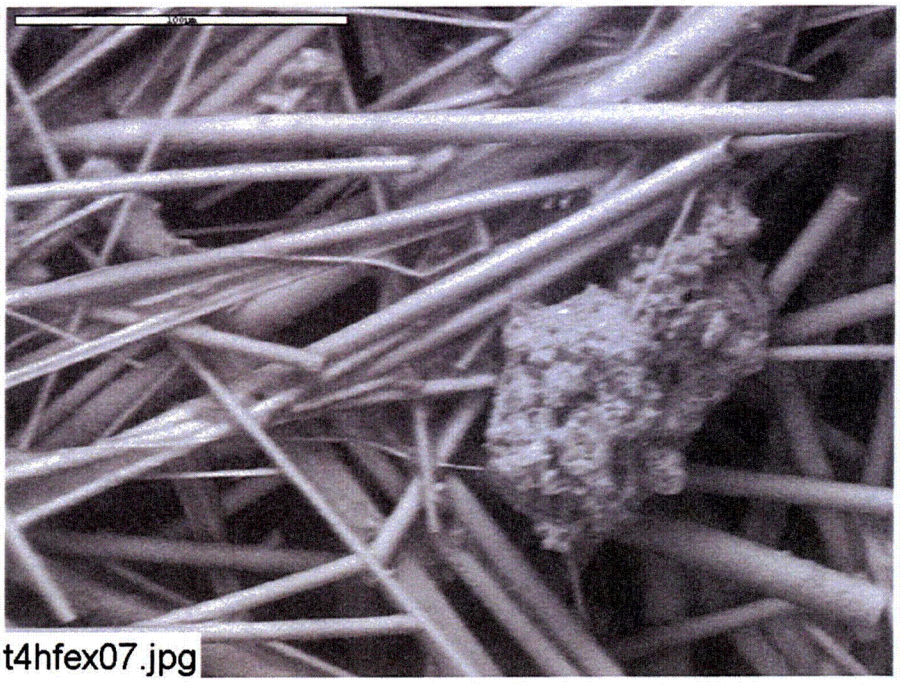

Figure 3-55. ESEM image magnified 500 times for a Test #4, Day-30 exterior high-flow fiberglass sample. (t4hfex07.jpg)

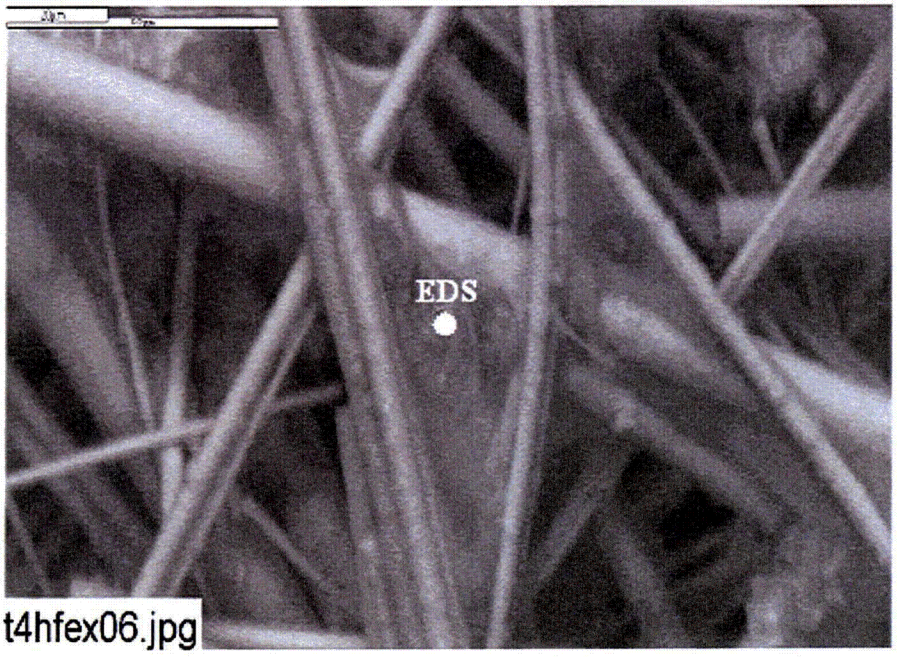

Figure 3-56. ESEM image magnified 800 times for a Test #4, Day-30 exterior high-flow fiberglass sample. (t4hfex06.jpg)

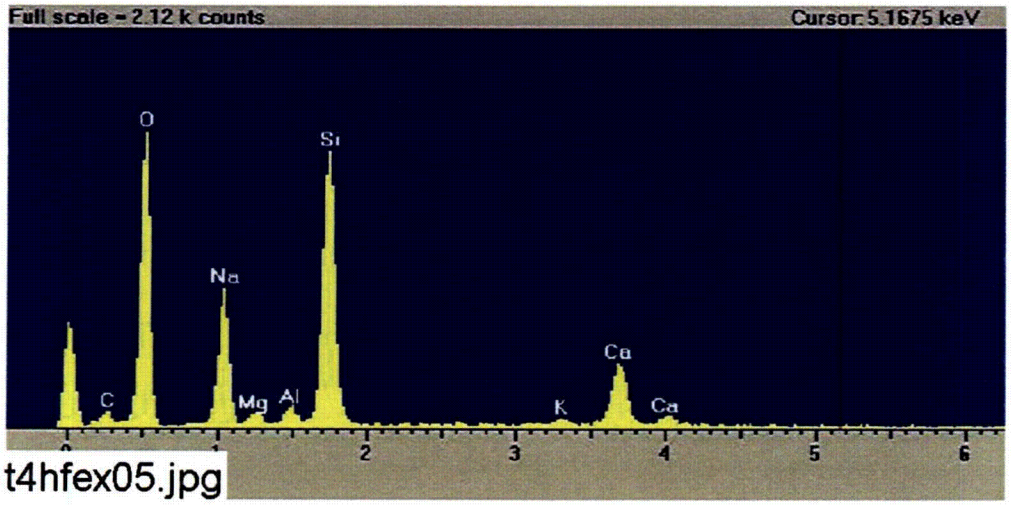

Figure 3-57. EDS counting spectrum for the spot of film on the fiberglass shown in Figure 3-56. (t4hfex05.jpg)

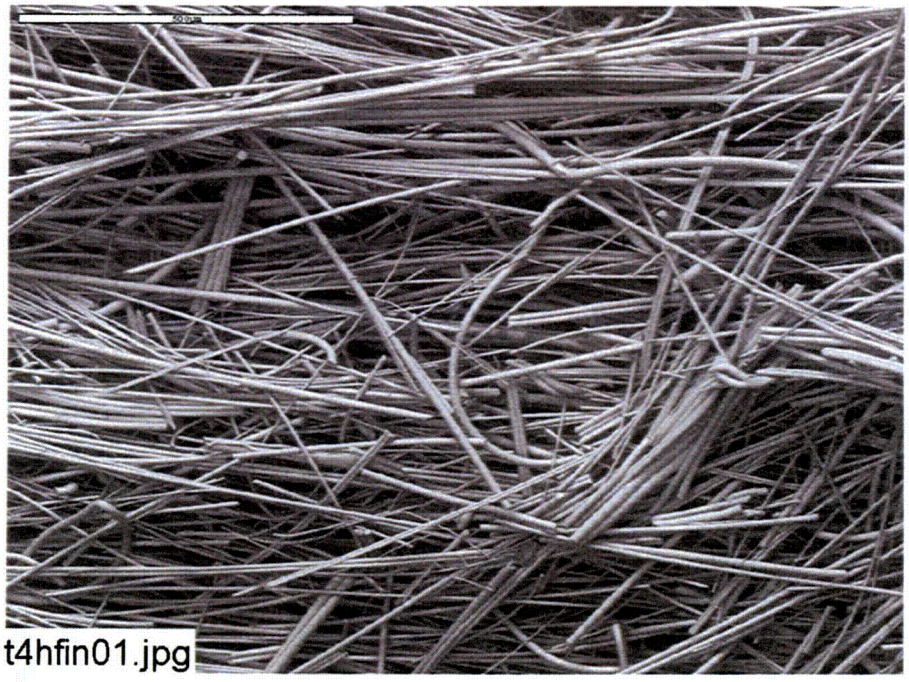

Figure 3-58. ESEM image magnified 100 times for a Test #4, Day-30 interior high-flow fiberglass sample. (t4hfin01.jpg)

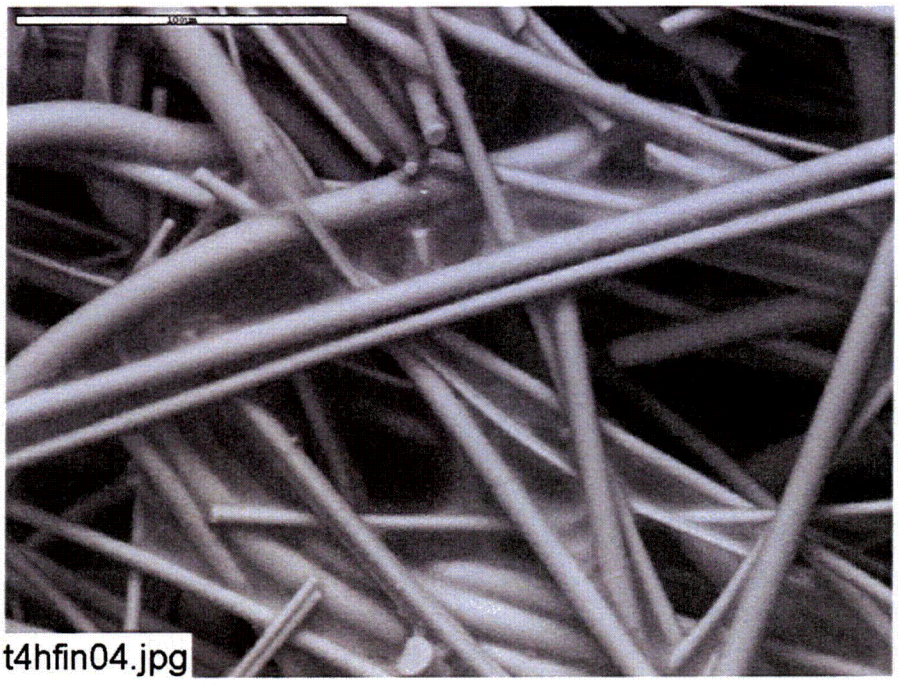

Figure 3-59. ESEM image magnified 500 times for a Test #4, Day-30 interior high-flow fiberglass sample. (t4hfin04.jpg)

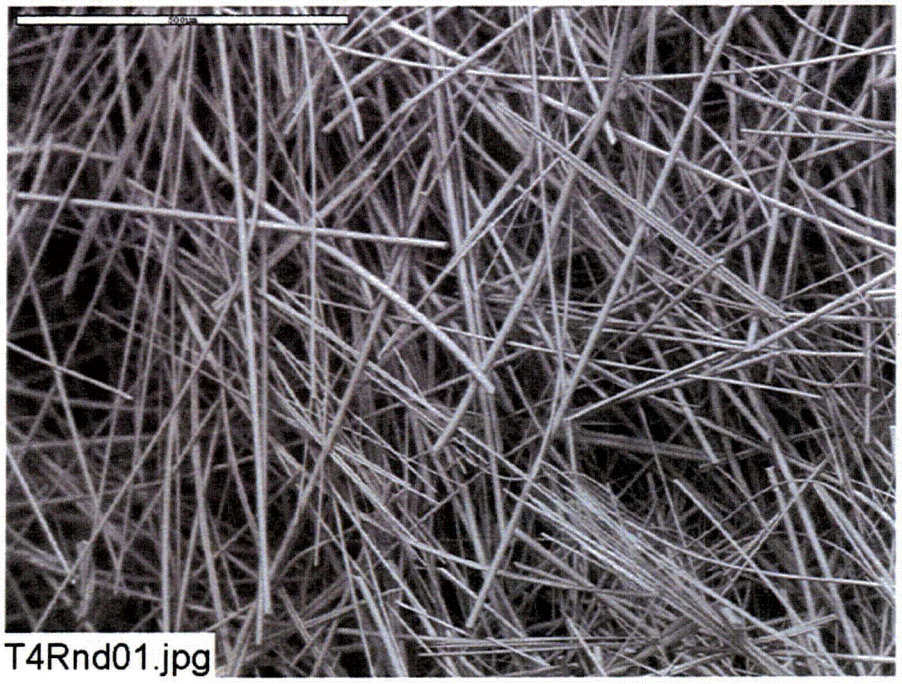

Figure 3-60. ESEM image magnified 100 times for a Test #4, Day-30 interior high-flow fiberglass sample. The sample was gently prerinsed with RO water. (T4Rnd01.jpg)

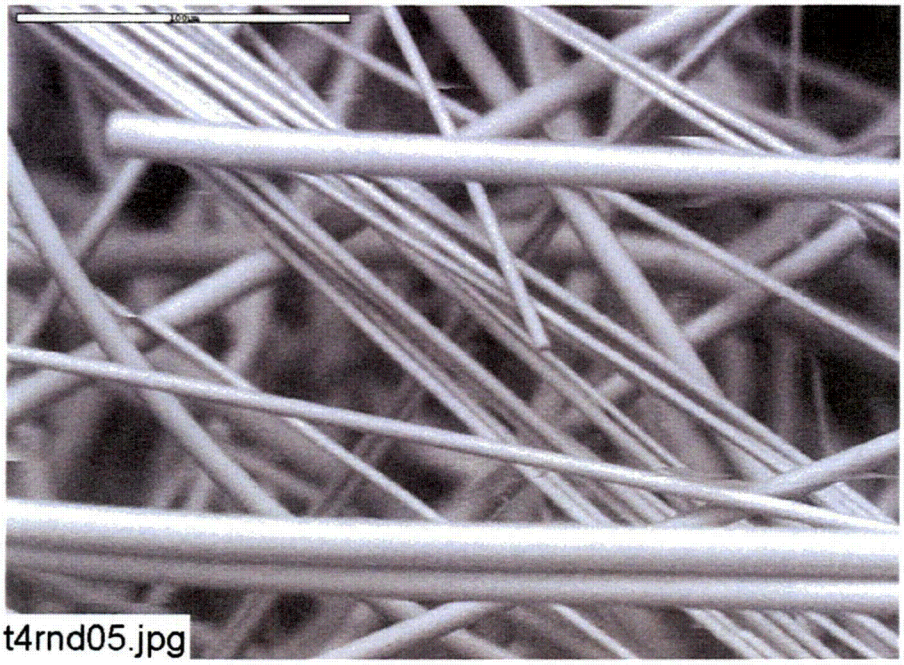

Figure 3-61. ESEM image magnified 500 times for a Test #4, Day-30 interior high-flow fiberglass sample. The sample was gently prerinsed with RO water. (t4rnd05.jpg)

3.3.1.8. Day-30 High-Flow Fiberglass Samples in Front of a Header

The images of the fiberglass in front of a header are different from the conventional high-flow fiberglass samples in Section 3.3.1.7. The header sample was put in the tank on Day 2 to compare with samples placed in the tank on Day 0. Due to settling of suspended particles and decrease in turbidity during the first two days of the test, no significant particulate deposits were found on the header fiberglass exterior, as shown by ESEM images. This suggests that the deposits observed on the exterior of the high-flow samples put in the tank on Day 0 are due to the higher suspended solids and turbidity present in the system during the first several days. However, the coating and film deposits were found on both the exterior and the interior of the header samples. Consistent with earlier observations, the coating and the film were composed of O, Na, Ca, Mg, Al, C, K, and possibly Si. As mentioned before, coating and film deposits are likely caused by chemical precipitation when the samples were partially dehydrated. Figures 3-62 through 3-68 show the results from the Day-30 high-flow fiberglass in front of a header.

Figure 3-62. ESEM image magnified 100 times for a Test #4, Day-30 exterior high-flow fiberglass sample in front of a header (inserted on Day 4). (t4d30hx1.jpg)

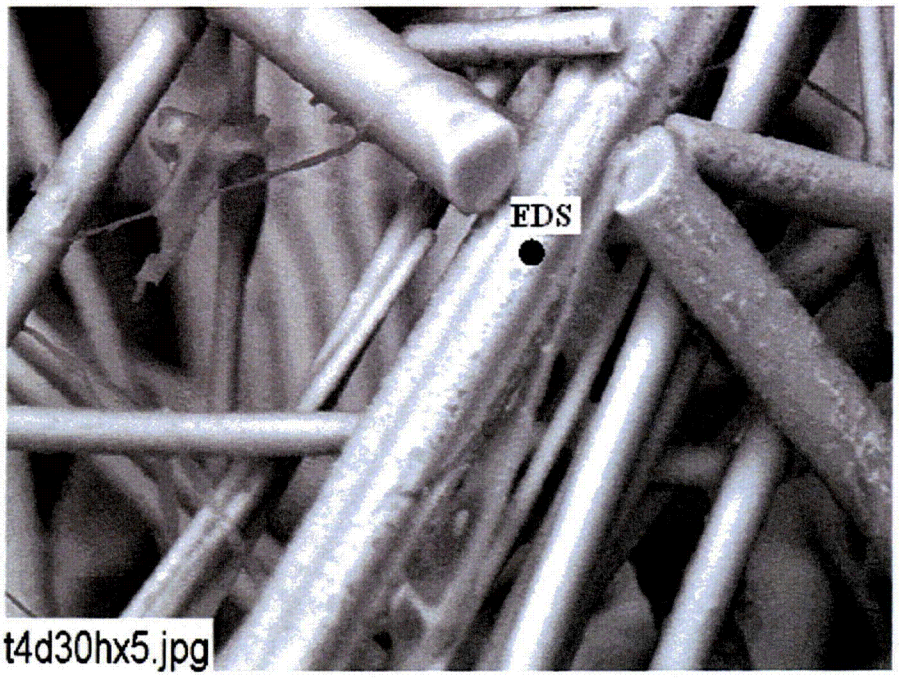

Figure 3-63. ESEM image magnified 1000 times for a Test #4, Day-30 exterior high-flow fiberglass sample in front of a header (inserted on Day 4). (t4d30hx5.jpg)

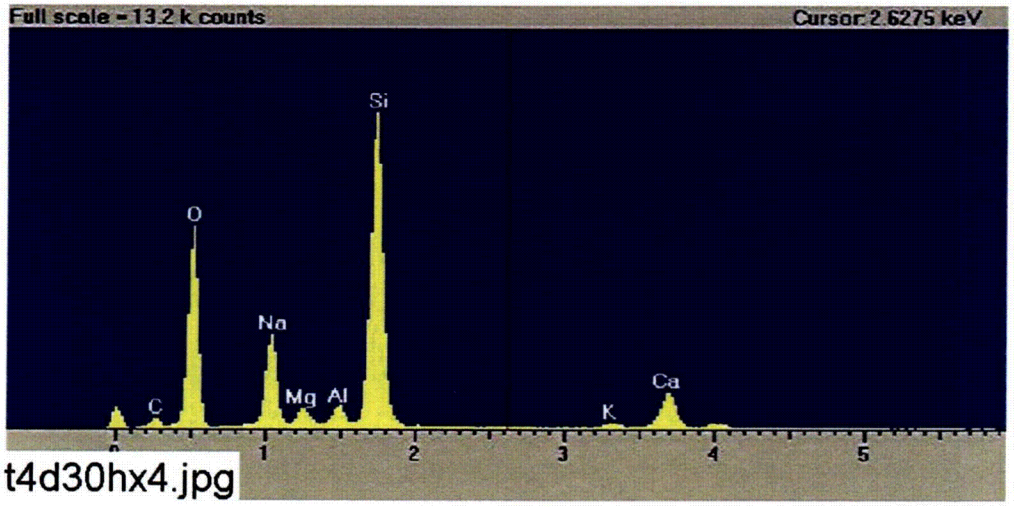

Figure 3-64. EDS counting spectrum for the spot of coating substance on fiberglass shown in Figure 3-63. (t4d30hx4.jpg)

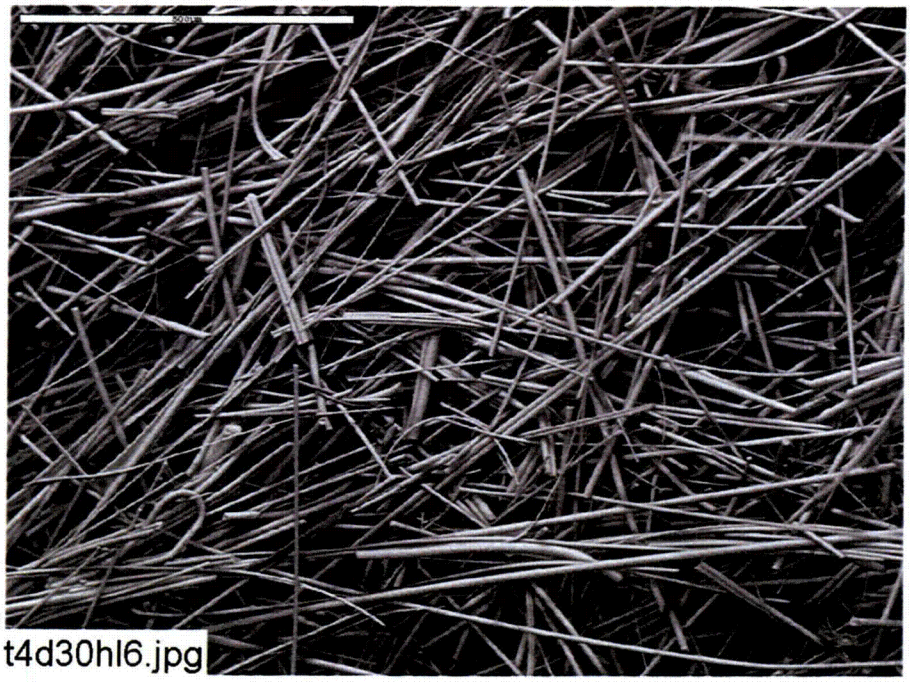

Figure 3-65. ESEM image magnified 100 times for a Test #4, Day-30 interior high-flow fiberglass sample in front of a header (inserted on Day 4). (t4d30hl6.jpg)

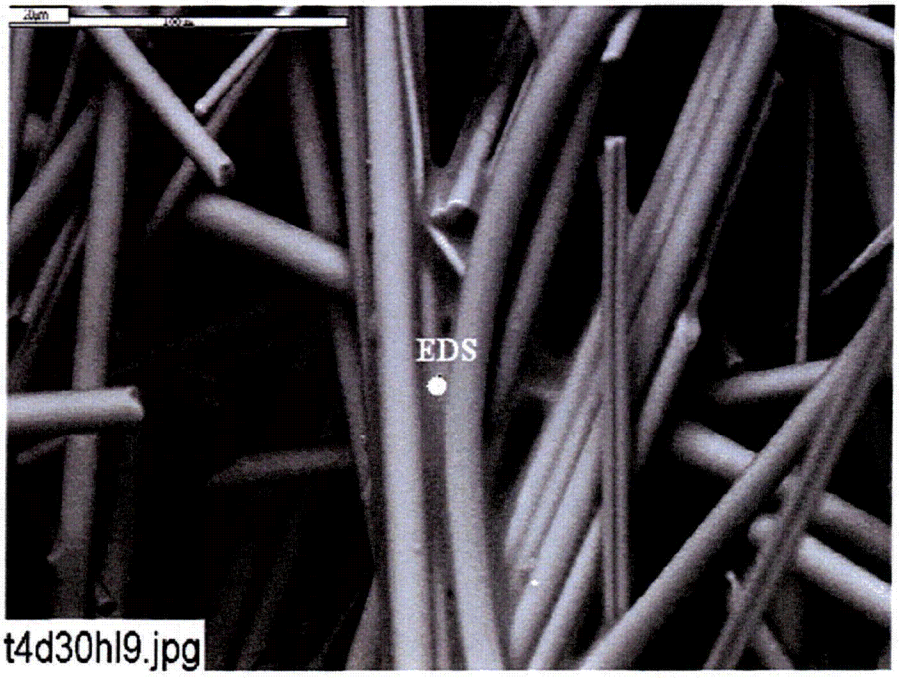

Figure 3-66. ESEM image magnified 500 times for a Test #4, Day-30 interior high-flow fiberglass sample in front of a header (inserted on Day 4). (t4d30hl9.jpg)

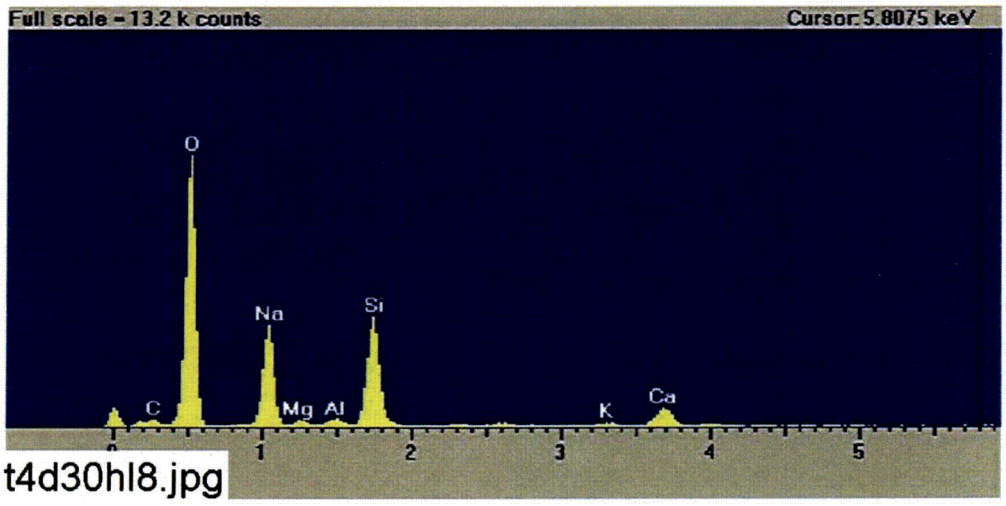

Figure 3-67. EDS counting spectrum for the spot of substance attached on fiberglass shown in Figure 3-66. (t4d30hl8.jpg)

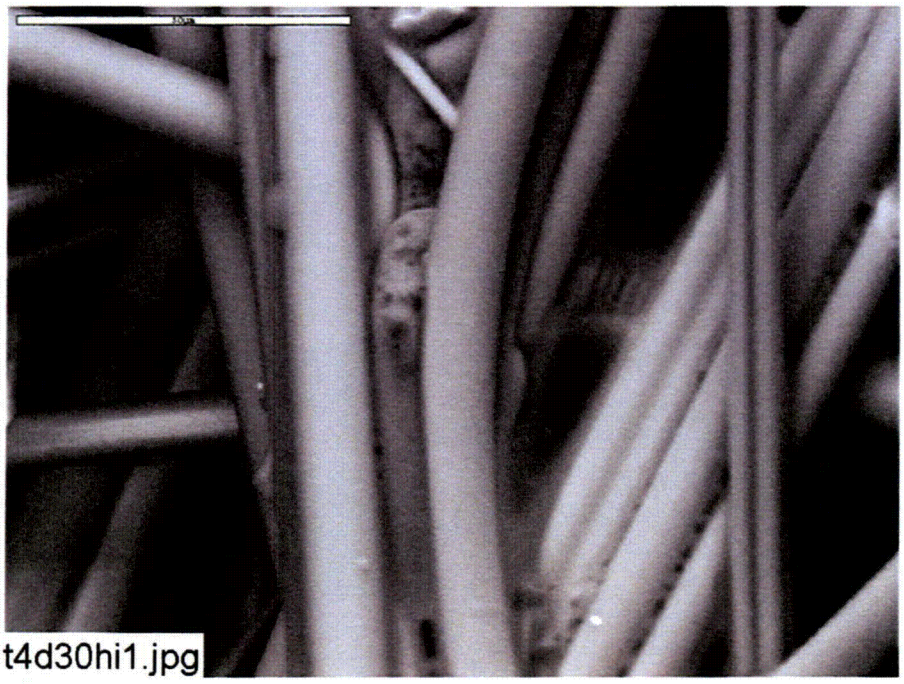

Figure 3-68. ESEM image magnified 1000 times for a Test #4, Day-30 interior high-flow fiberglass sample in front of a header (inserted on Day 4). (t4d30hi1.jpg)

3.3.1.9. Day-30 Drain Collar Fiberglass Samples

When the tank was drained, the drain collar was totally surrounded by sediment. Figure 3-121 shows the drain collar after the tank was drained. Both the exterior fiberglass sample that was farthest from the drain screen and the exterior sample that was next to the drain screen have significant amounts of particulate deposits. Inspection revealed the development of a continuous coating on the drain collar exterior, including particulate deposits that were likely physically retained or attached. The amount of deposits on the drain collar exterior was greater than on high- and low-flow fiberglass samples. EDS results indicate that the particulate deposits were mainly composed of O, Si, Ca, Na, Al, and C, regardless of whether the drain collar exterior was farthest from the drain screen or next to the drain screen. The high content of Si and Ca in the particulate deposits suggests that they were probably from cal-sil debris. In contrast to the exterior, no significant particulate deposits were found in the drain collar interior sample, and only film-like deposits were found (see Figure 3-75). The drain collar interior appears similar to the other high- and low- flow fiberglass interior samples. This result suggests that almost all of the particulate deposits were physically retained at the fiberglass exterior, which is consistent with Day-30 high-flow fiberglass samples. Figures 3-69 through 3-79 show the drain collar fiberglass results.

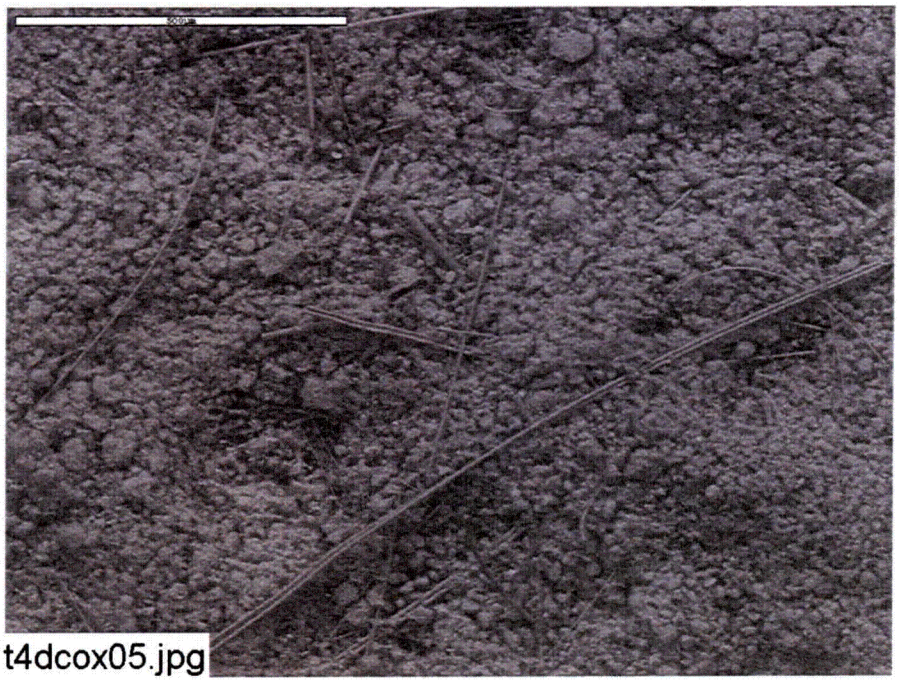

Figure 3-69. ESEM image magnified 100 times for a Test #4, Day-30 exterior fiberglass sample on the drain collar (away from the drain screen). (t4dcox05.jpg)

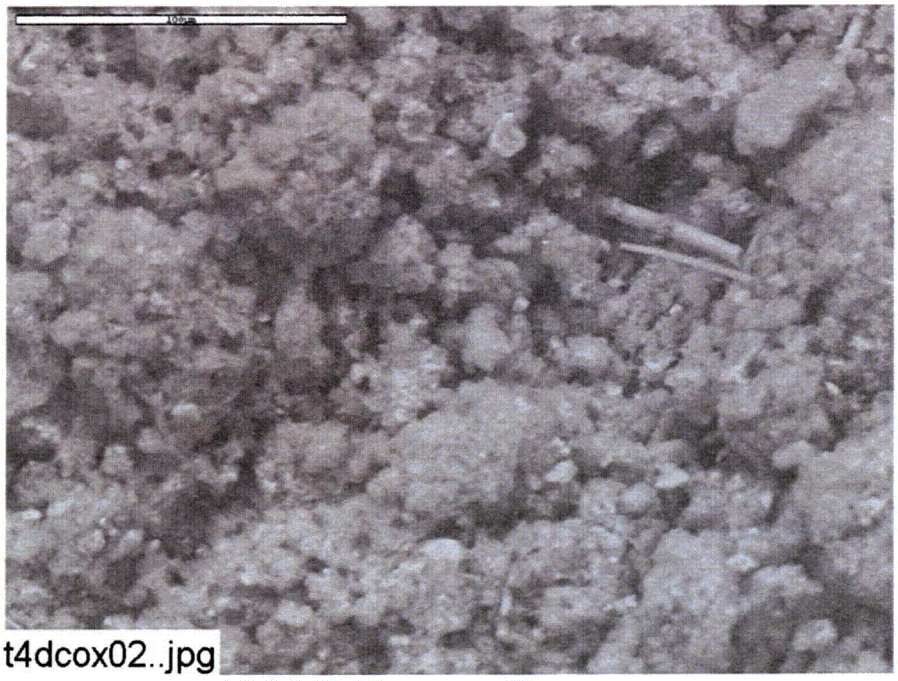

Figure 3-70. ESEM image magnified 500 times for a Test #4, Day-30 exterior fiberglass sample on the drain collar (away from the drain screen). (t4dcox02.jpg)

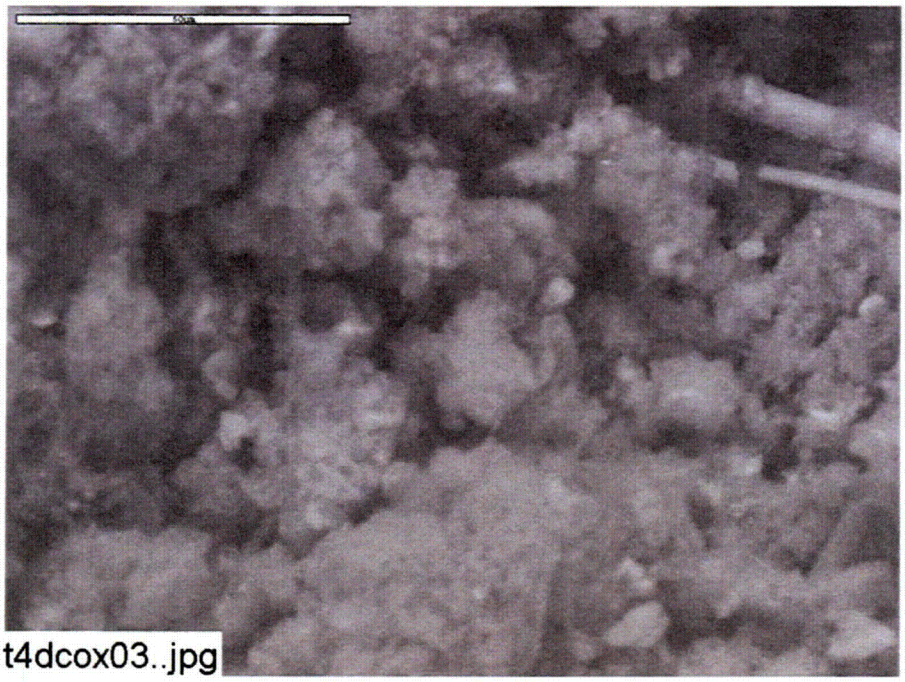

Figure 3-71. ESEM image magnified 1000 times for a Test #4, Day-30 exterior fiberglass sample on the drain collar (away from the drain screen). (t4dcox03.jpg)

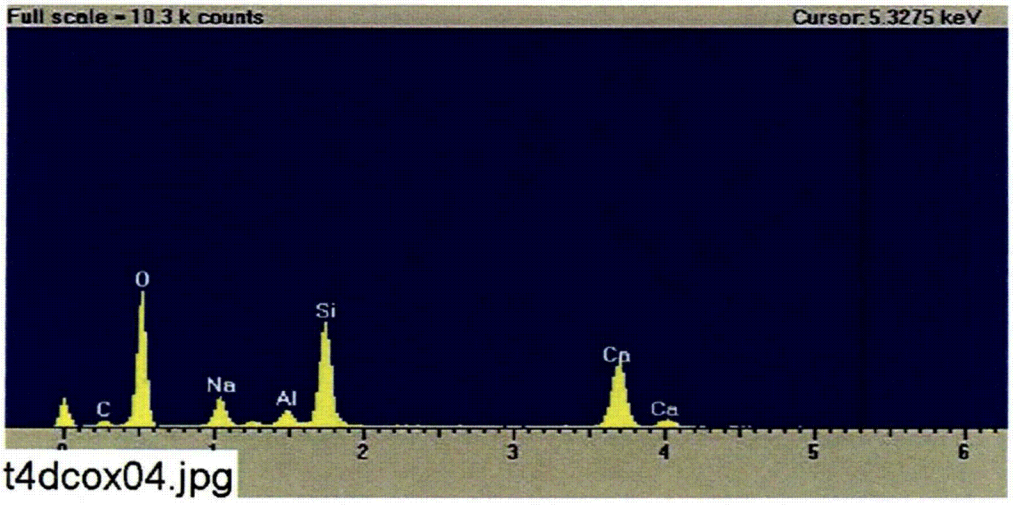

Figure 3-72. EDS counting spectrum for the large mass of particulate deposits on fiberglass shown in Figure 3-71. (t4dcox04.jpg)

Figure 3-73. ESEM image magnified 100 times for a Test #4, Day-30 interior fiberglass sample on the drain collar. (t4dcin11.jpg)

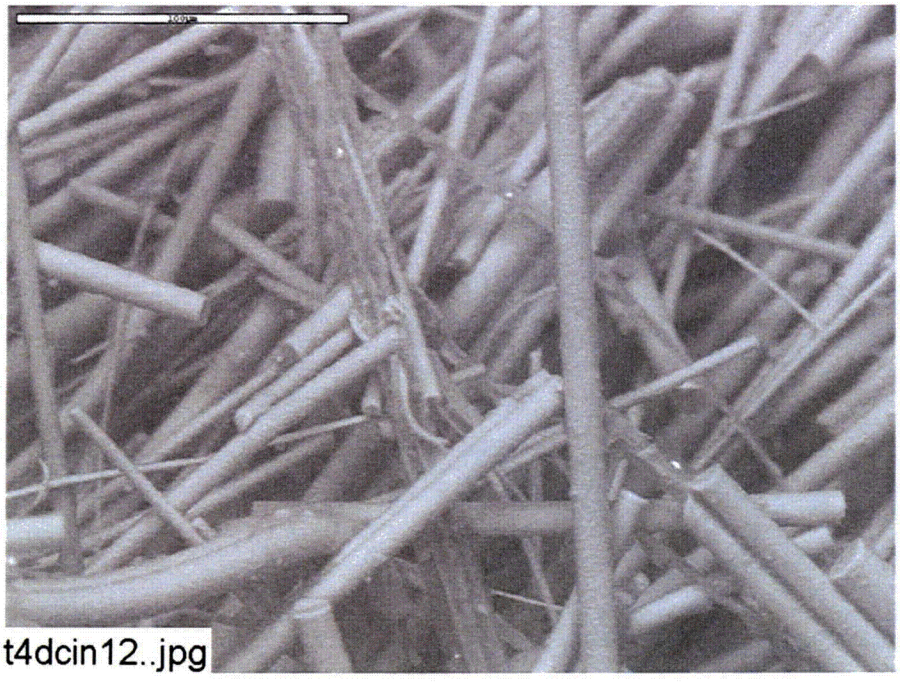

Figure 3-74. ESEM image magnified 500 times for a Test #4, Day-30 interior fiberglass sample on the drain collar. (t4dcin12.jpg)

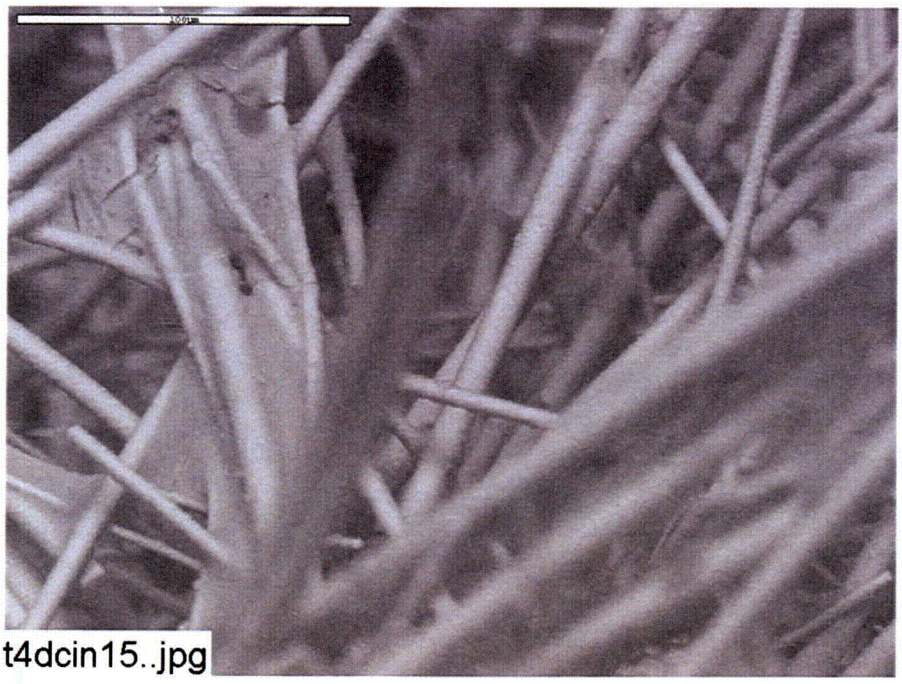

Figure 3-75. ESEM image magnified 500 times for a Test #4, Day-30 interior fiberglass sample on the drain collar. (t4dcin15.jpg)

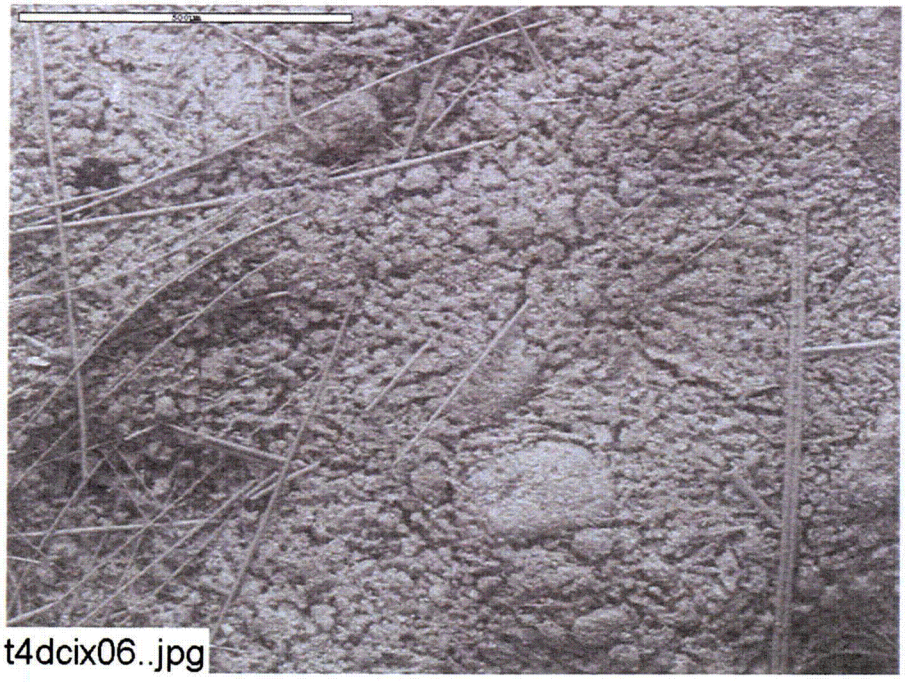

Figure 3-76. ESEM image magnified 100 times for a Test #4, Day-30 exterior fiberglass sample on the drain collar (next to the drain screen). (t4dcix06.jpg)

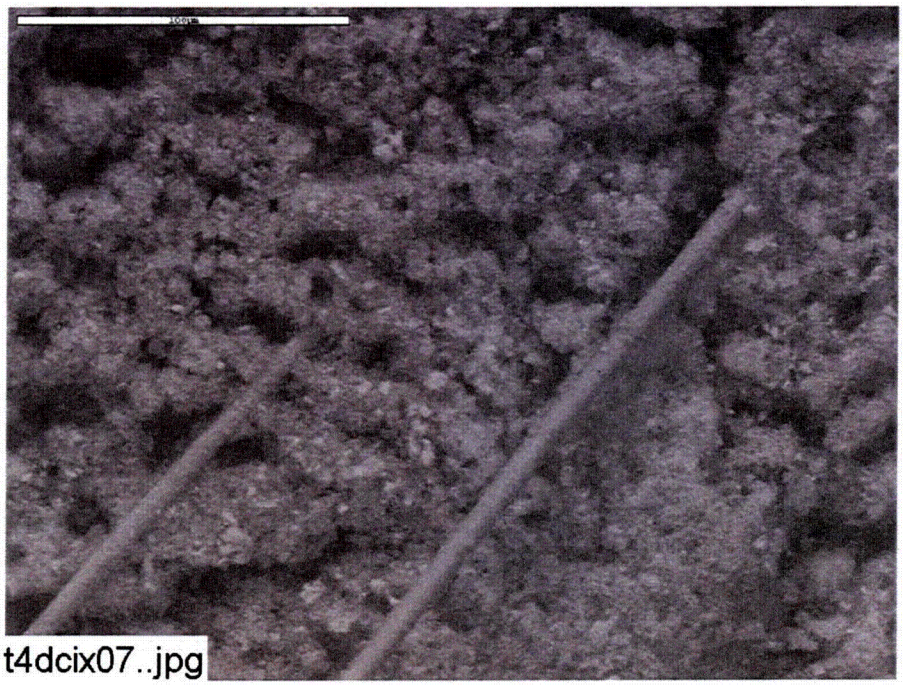

Figure 3-77. ESEM image magnified 500 times for a Test #4, Day-30 exterior fiberglass sample on the drain collar (next to the drain screen). (t4dcix07.jpg)

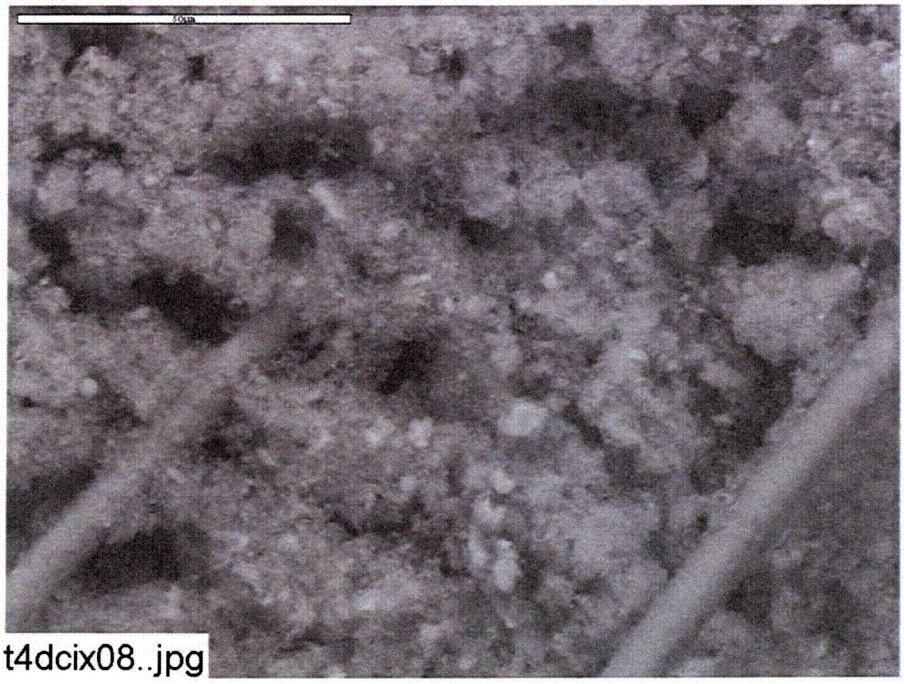

Figure 3-78. ESEM image magnified 1000 times for a Test #4, Day-30 exterior fiberglass sample on the drain collar (next to the drain screen). (t4dcix08.jpg)

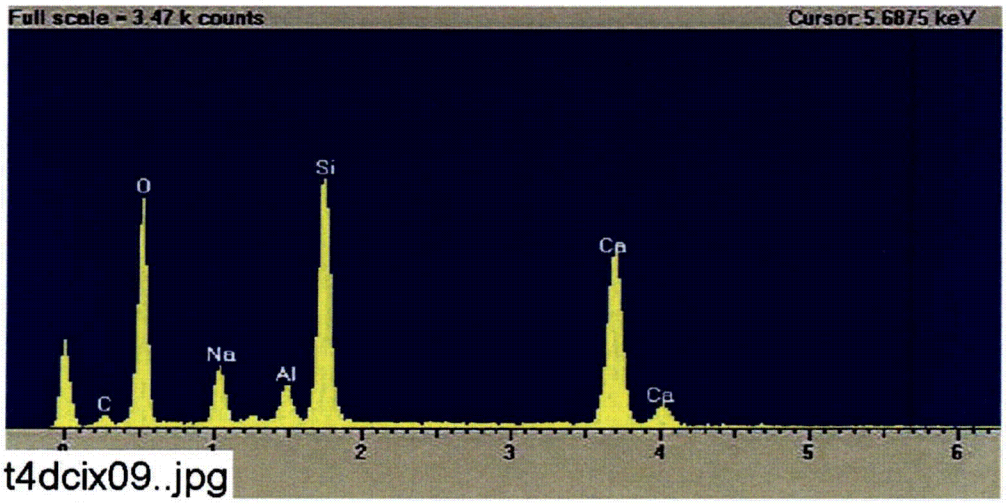

Figure 3-79. EDS counting spectrum for the large mass of particulate deposits on fiberglass shown in Figure 3-78. (t4dcix09.jpg)

3.3.1.10. Day-30 Fiberglass Sample within the Birdcage

For the Day-30 fiberglass sample within the birdcage, the SEM images indicate a significant amount of particulate deposits (see Figure 3-80) on the exterior of the fiberglass. The location of the birdcage was on top of a large cal-sil sample that sat on the bottom of the tank and was in direct contact with the sediment. The birdcage, however, was not in direct contact with the sediment. The amount of particulate deposits was greater than the amounts on the high- and low-flow fiberglass samples, but less than the drain collar exterior. The EDS result shows that the particulate deposits were composed of O, Si, Ca, Na, Al, and C, which is consistent with the drain collar exterior. Again, the high content of Si and Ca suggests these particulate deposits were from cal-sil debris. Compared to the exterior, the interior sample was relatively clean. Only film deposits were found. These film deposits were similar to the observed high- and low-flow fiberglass samples, which were likely caused by chemical precipitation during the drying process. Again, this result suggests that almost all of the particulate deposits were physically retained at the fiberglass exterior, consistent with Day-30 high-flow and drain collar fiberglass samples. Figures 3-80 through 3-85 show the birdcage fiberglass results.

Figure 3-80. ESEM image magnified 100 times for a Test #4, Day-30 exterior fiberglass sample within the birdcage. (T4D30BX1.jpg)

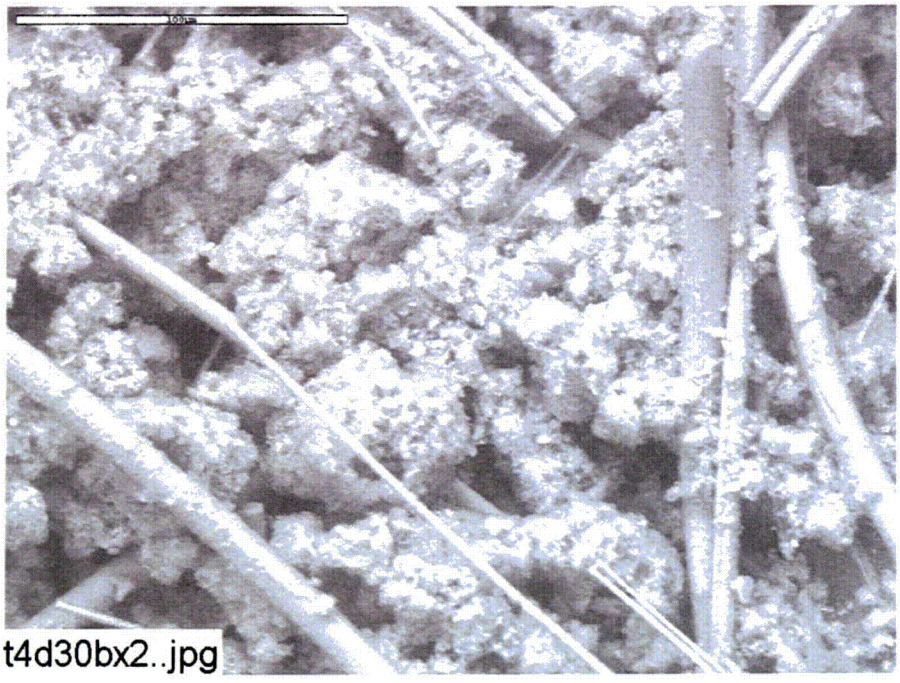

Figure 3-81. ESEM image magnified 500 times for a Test #4, Day-30 exterior fiberglass sample within the birdcage. (T4D30bx2.jpg)

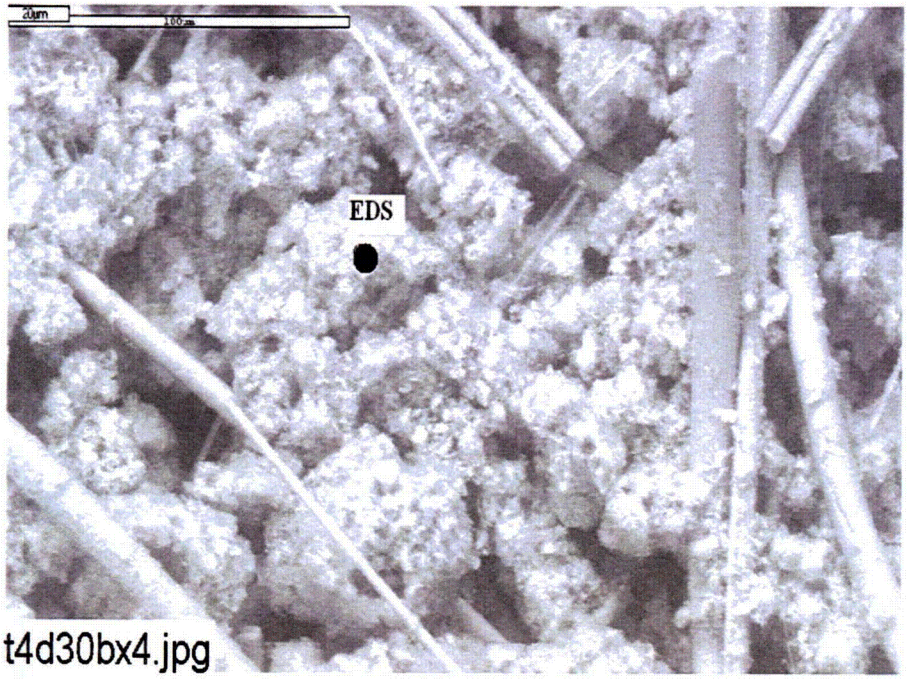

Figure 3-82. Annotated ESEM image magnified 500 times for a Test #4, Day-30 exterior fiberglass sample within the birdcage. (t4d30bx4.jpg)

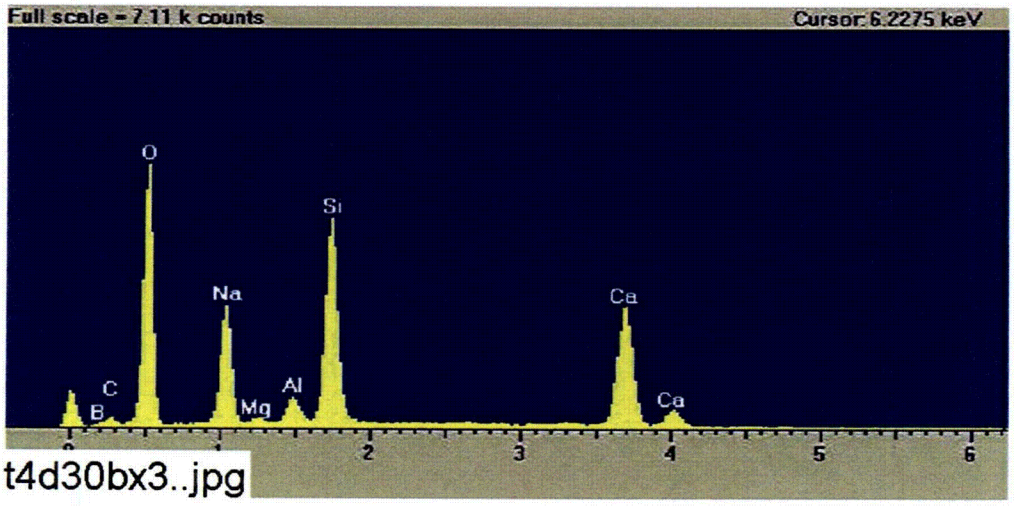

Figure 3-83. EDS counting spectrum for the particulate deposits on fiberglass shown in Figure 3-82. (T4D30bx3.jpg)

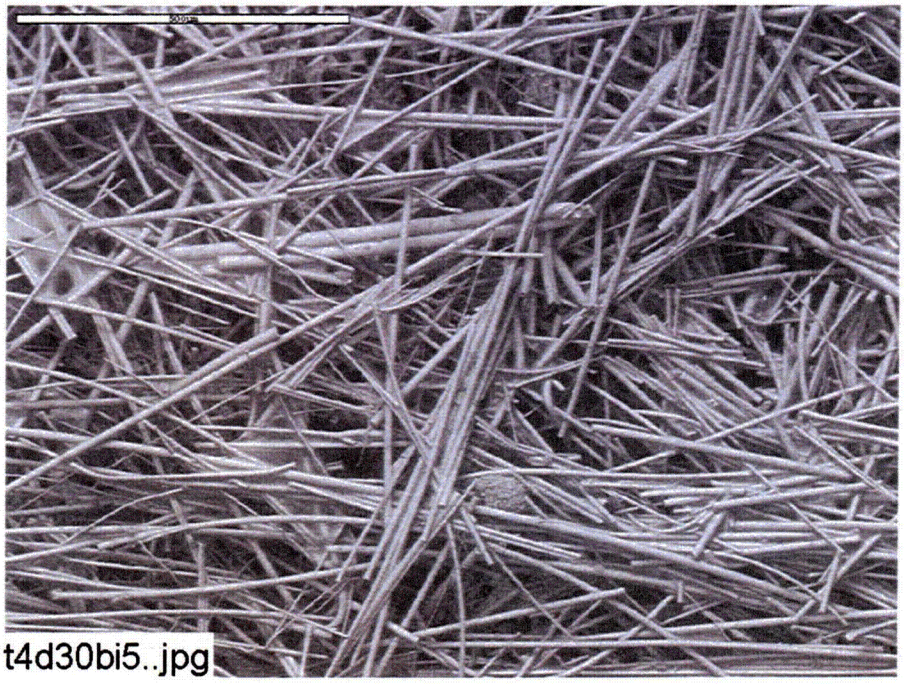

Figure 3-84. ESEM image magnified 100 times for a Test #4, Day-30 interior fiberglass sample within the birdcage. (t4d30bi5.jpg)

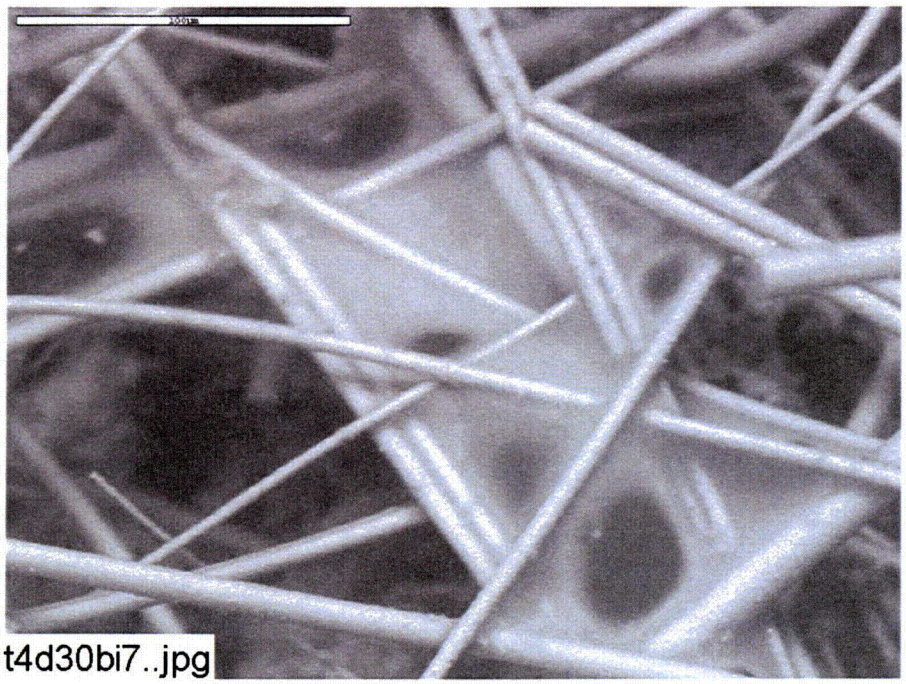

Figure 3-85. ESEM image magnified 500 times for a Test #4, Day-30 interior fiberglass sample within the birdcage. (t4d30bi7.jpg)

3.3.2. Calcium Silicate Samples

ICET Test #4 was the second test that included cal-sil insulation samples in addition to fiberglass samples. XRD/XRF results show the crystal structure and the chemical composition of the unused raw and unused baked cal-sil samples. Based on XRD results, both unused raw and unused baked cal-sil samples contained crystalline substances of tobermorite ($Ca_{2.25}(Si_3O_{7.5}(OH)_{1.5})(H_2O)$) and calcite ($CaCO_3$). XRF results indicated that the dominant elemental compositions of cal-sil include Si and Ca and small amounts of Al, Fe, Na, and Mg. There was no significant difference in elemental composition between raw and baked unused cal-sil. After being baked in a laboratory oven at 260°C for 72 hours, the raw cal-sil color changed from yellow to pink. The possible property changes of cal-sil after being baked include loss of water and oxidation of reductive species such as organic carbon, Fe(0), and Fe(II), as well as possible mineral and crystal structural changes. Specifically, oxidation of Fe(0) and Fe(II) into Fe_2O_3 is likely responsible for the baked cal-sil's turning pink.

Both raw and baked cal-sil samples were submerged in the tank throughout the test. No significant differences were found between the raw and baked cal-sil, or between the exterior and the interior. EDS results show that both raw and baked cal-sil were composed primarily of O, Si, Ca, Na, Al, C, Mg, and Fe. Due to the granular shape of cal-sil particles, it is difficult to distinguish whether the particles are foreign deposits or they are the cal-sil particles themselves. Figures 3-86 through 3-97 show cal-sil results.

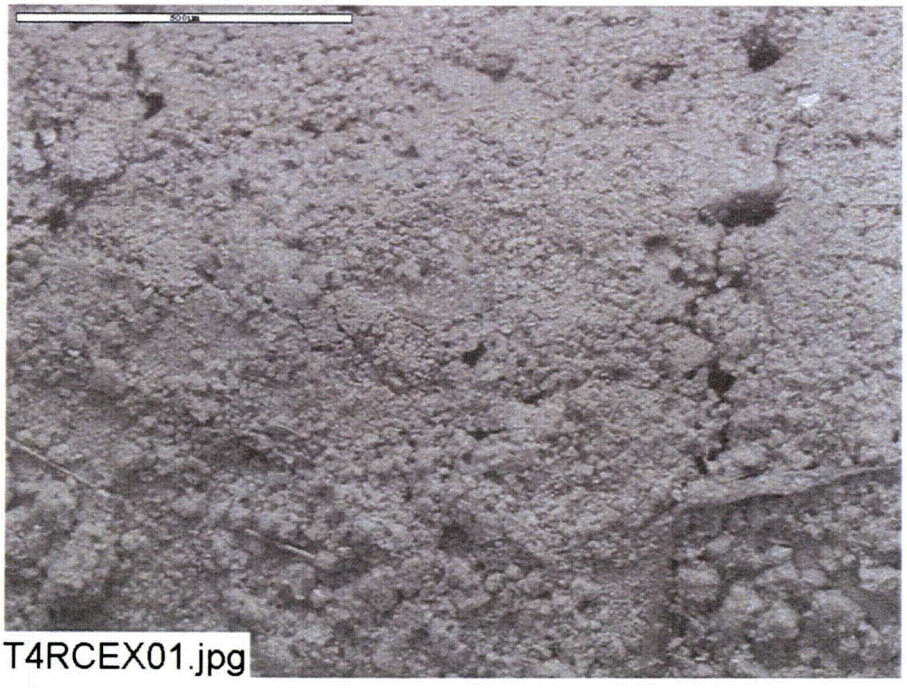

Figure 3-86. ESEM image magnified 100 times for a Test #4, Day-30 low-flow exterior raw cal-sil sample. (T4RCEX01.jpg)

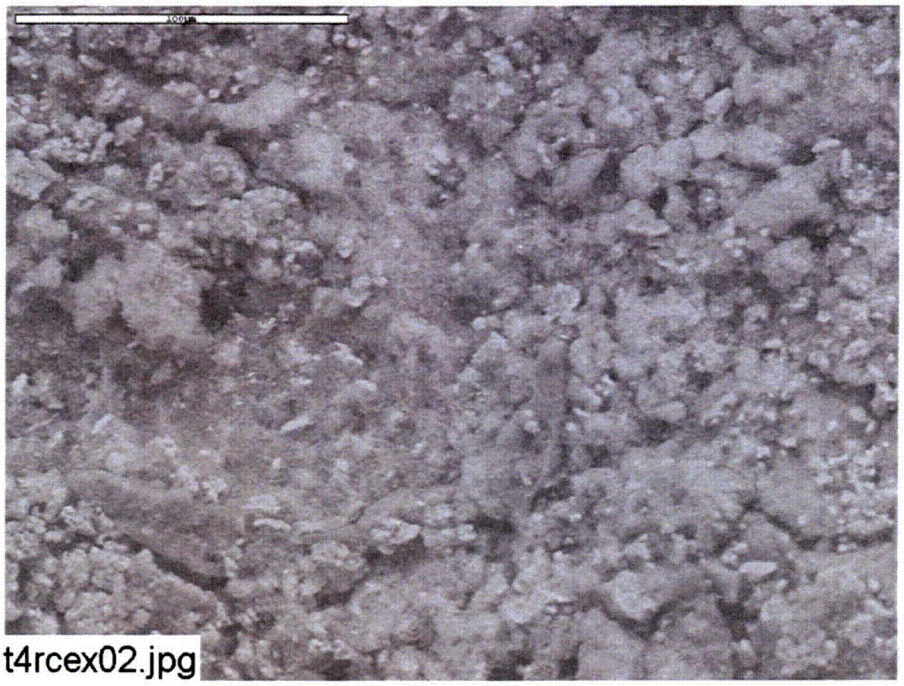

Figure 3-87. ESEM image magnified 500 times for a Test #4, Day-30 low-flow exterior raw cal-sil sample. (t4rcex02.jpg)

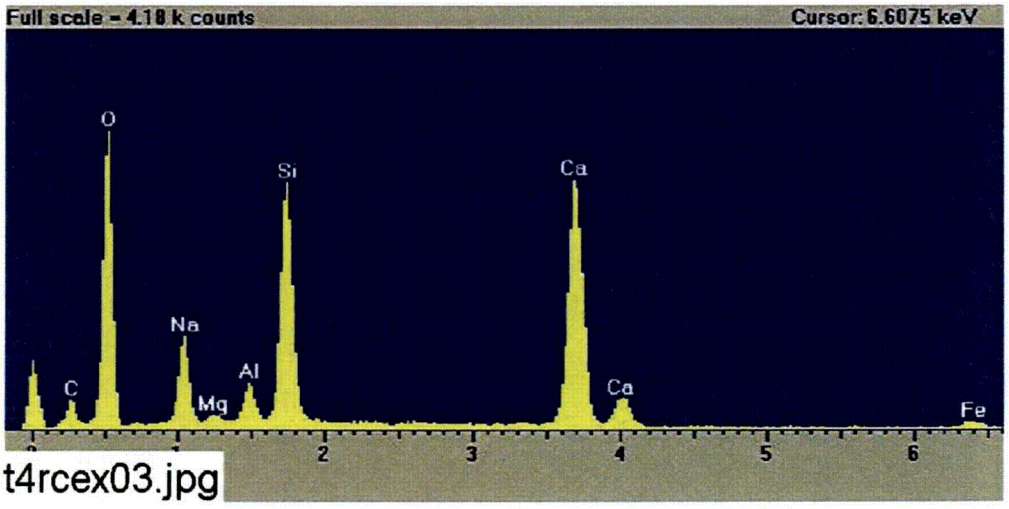

Figure 3-88. EDS counting spectrum for the whole image shown in Figure 3-87. (t4rcex03.jpg)

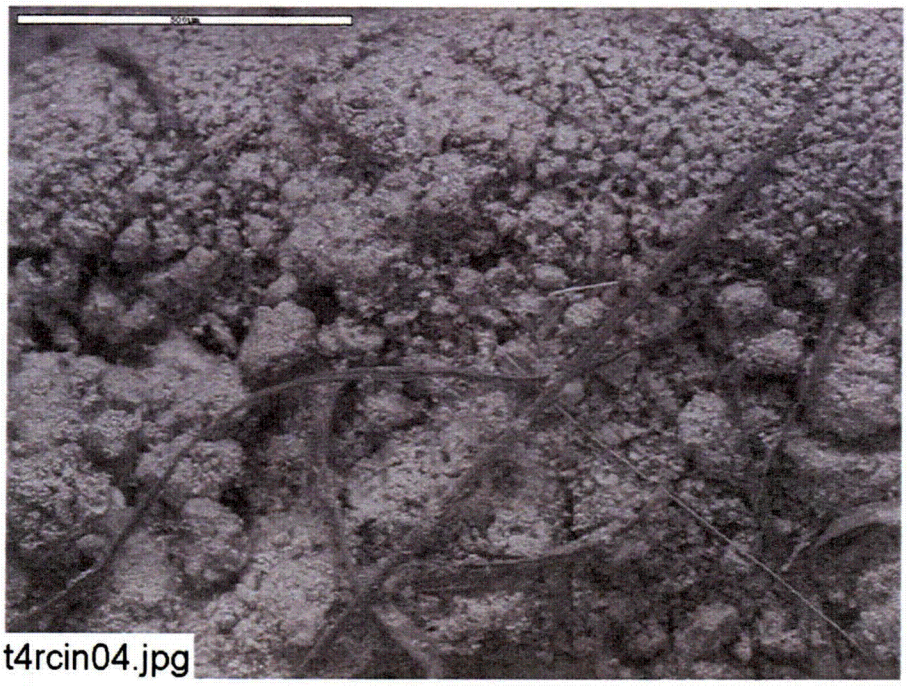

Figure 3-89. ESEM image magnified 100 times for a Test #4, Day-30 low-flow interior raw cal-sil sample. (t4rcin04.jpg)

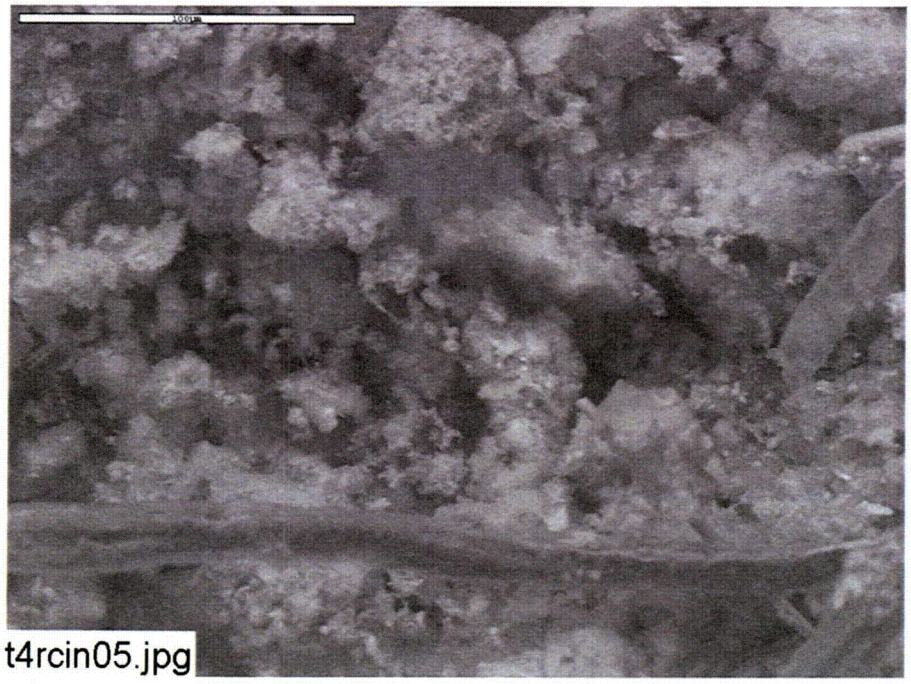

Figure 3-90. ESEM image magnified 500 times for a Test #4, Day-30 low-flow interior raw cal-sil sample. (t4rcin05.jpg)

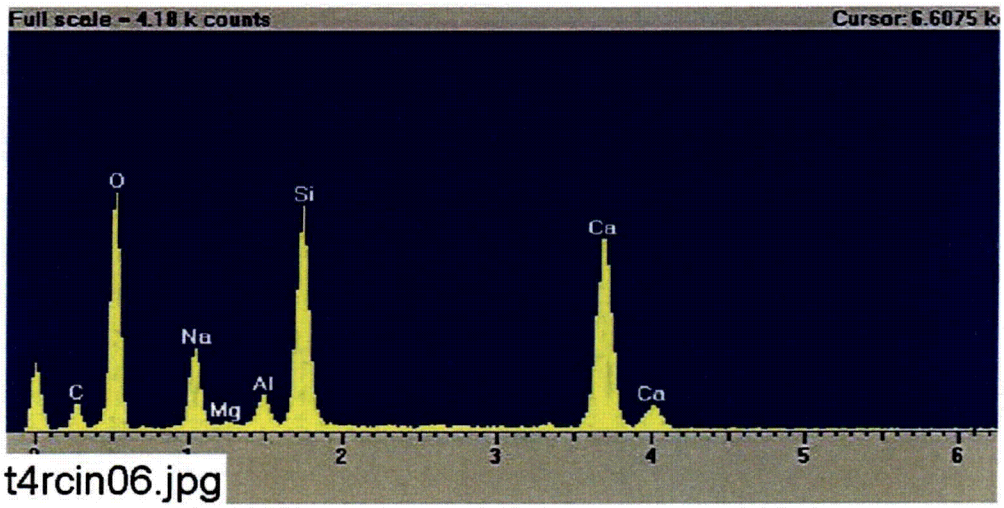

Figure 3-91. EDS counting spectrum for the whole image shown in Figure 3-90. (t4rcin06.jpg)

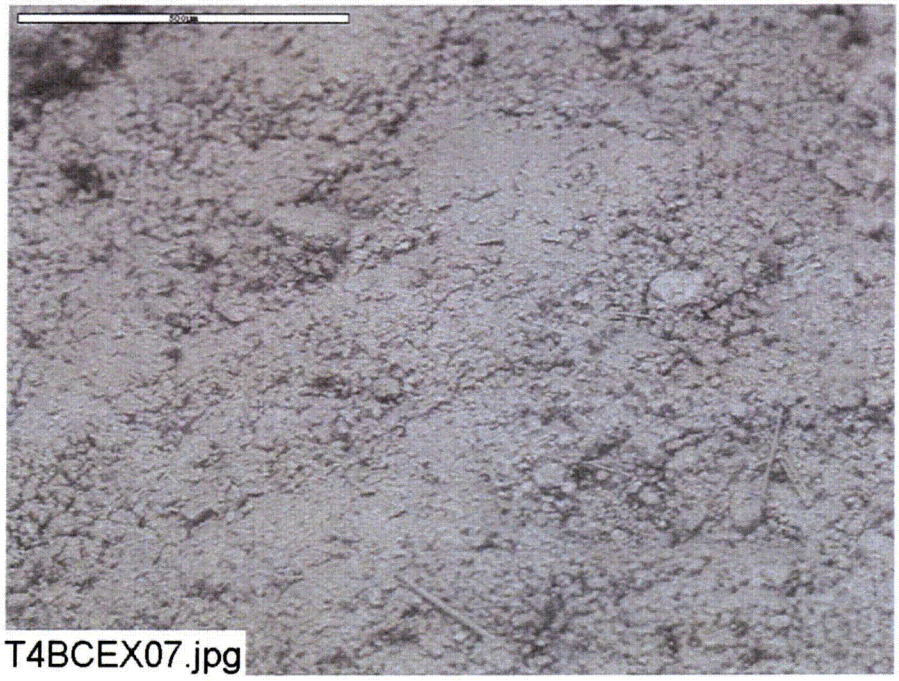

Figure 3-92. ESEM image magnified 100 times for a Test #4, Day-30 low-flow exterior baked cal-sil sample. (T4BCEX07.jpg)

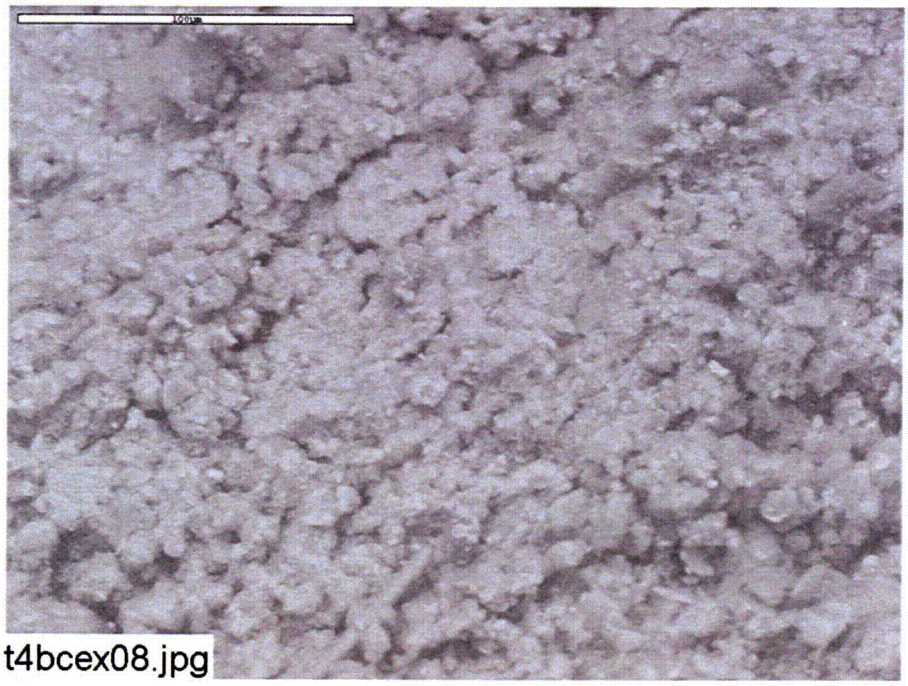

Figure 3-93. ESEM image magnified 500 times for a Test #4, Day-30 low-flow exterior baked cal-sil sample. (t4bcex08.jpg)

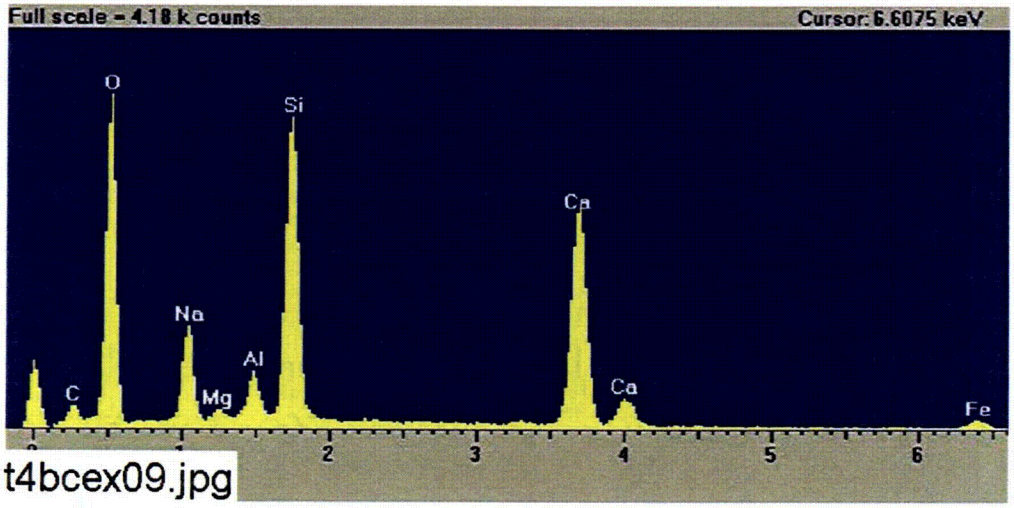

Figure 3-94. EDS counting spectrum for the whole image shown in Figure 3-93. (t4bcex09.jpg)

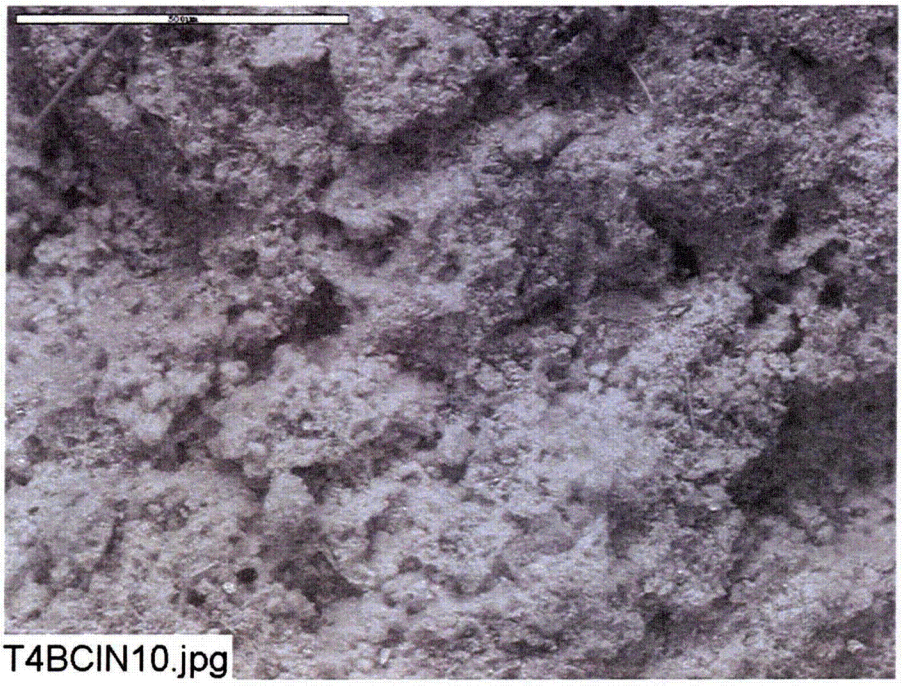

Figure 3-95. ESEM image magnified 100 times for a Test #4, Day-30 low-flow interior baked cal-sil sample. (T4BCIN10.jpg)

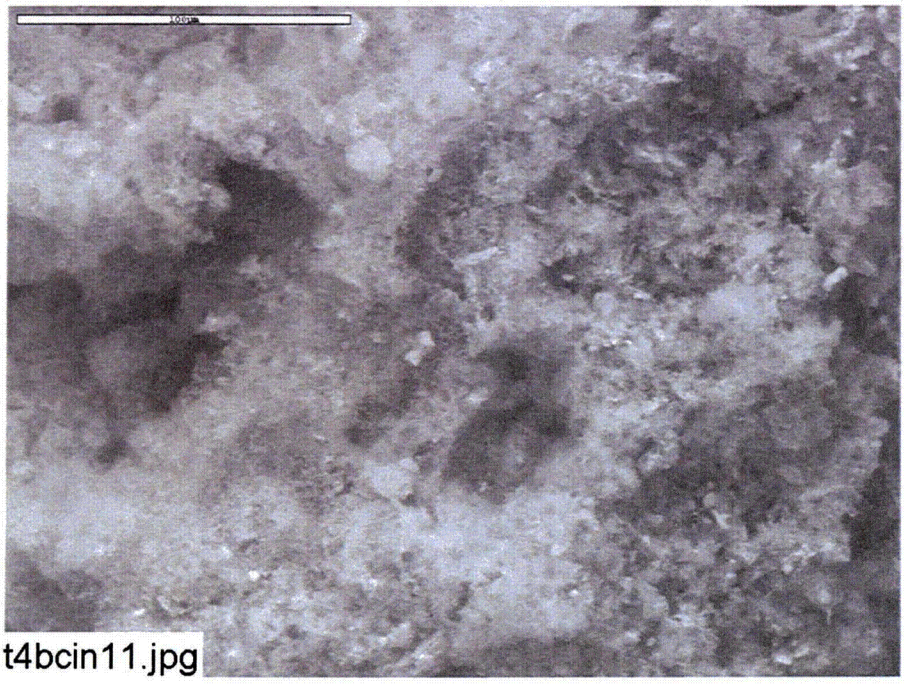

Figure 3-96. ESEM image magnified 500 times for a Test #4, Day-30 low-flow interior baked cal-sil sample. (t4bcin11.jpg)

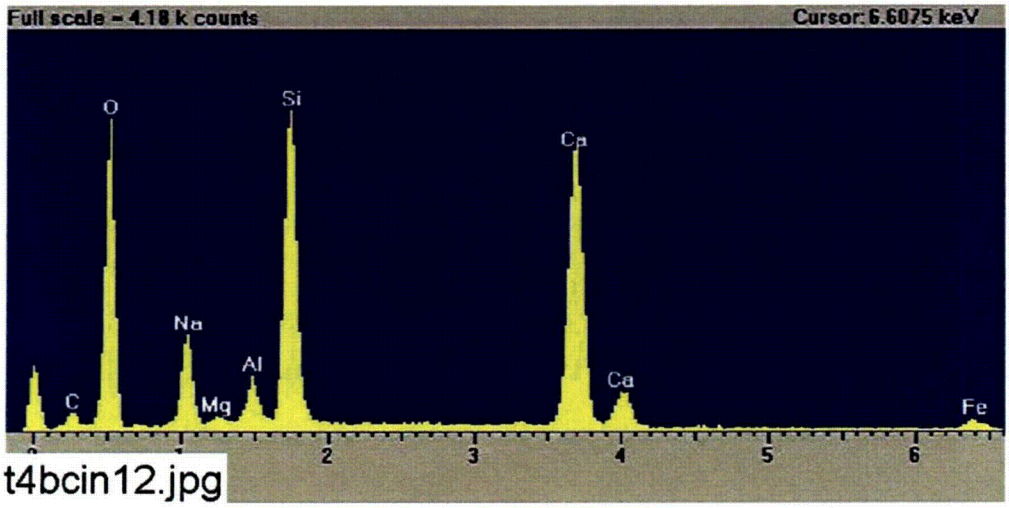

Figure 3-97. EDS counting spectrum for the whole image shown in Figure 3-95. (t4bcin12.jpg)

3.4. Metallic and Concrete Coupons

3.4.1. Weights and Visual Descriptions

3.4.1.1. Submerged Coupons

Examination of the 40 submerged coupons provides insights into the nature of the chemical kinetics that occurred during this 30-day test. The physical change that these coupons experienced is determined through both visual evidence and weight measurement of each coupon before and after the test. Pre-test pictures were taken of the coupons when they were received and before insertion in the racks. Post-test pictures were taken several days after the racks had been removed from the tank. All racks with coupons still inserted were staged to allow complete drying of the coupons before the post-test pictures. The coupons were placed in a low-humidity room and allowed to air dry. All coupons were also weighed before they were inserted into the tank and after the 30-day test was completed.

There are three submerged aluminum coupons in each test. Figures 3-98 through 3-100 display the pre- and post-test pictures of those coupons that were in Test #4. The relative locations of the aluminum coupons from east to west of the tank are: Al-239, Al-238, and Al-237. Al-239 and Al-238 were the two aluminum coupons that were isolated next to the concrete coupon. There were no visual differences between the three coupons after they were removed from the tank. The overall appearance of the aluminum coupons did not significantly change from their pre-test appearance. The post-test coupons appeared to have a light film on them and had lost their pre-test shiny appearance.

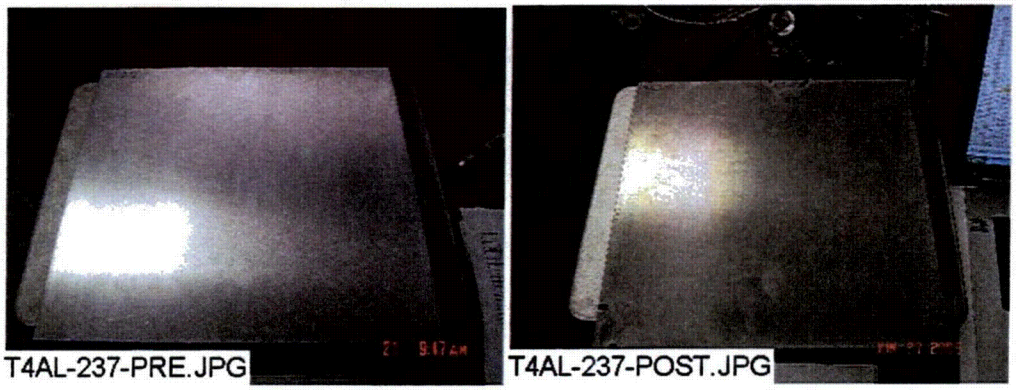

Figure 3-98. Al-237 submerged, pre-test (left) and post-test (right).

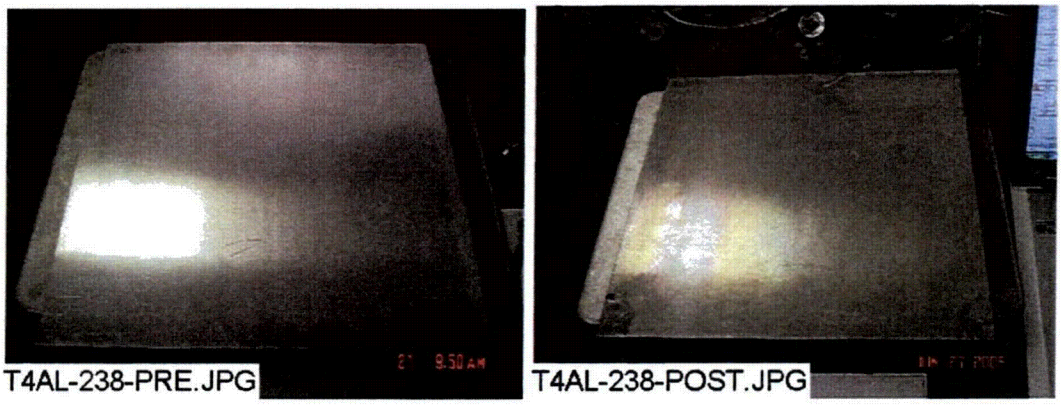

Figure 3-99. Al-238 submerged, pre-test (left) and post-test (right).

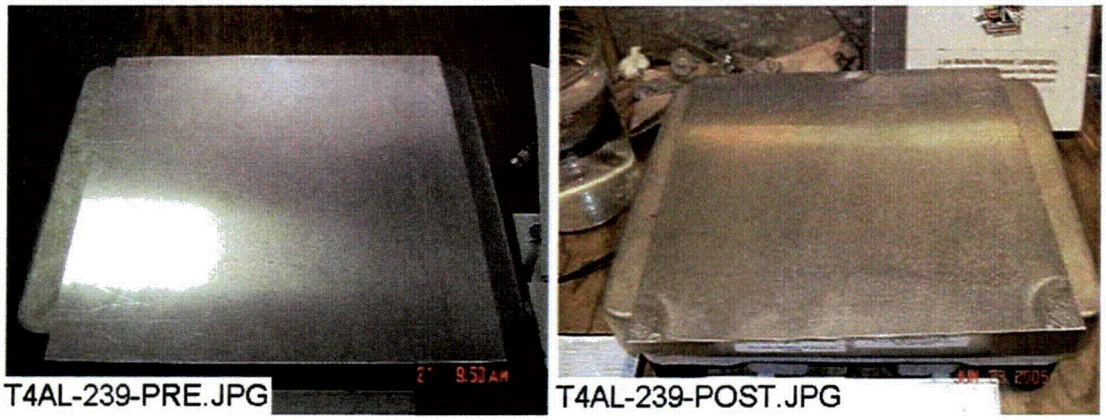

Figure 3-100. Al-239 submerged, pre-test (left) and post-test (right).

Figures 3-101 through 3-103 present the pre- and post-test pictures of three submerged galvanized steel coupons. The galvanized steel coupons did not experience any significant observable change. The coupons appeared to be relatively clean and the only noticeable marks of any sort are the circular marks caused by the racks that they are mounted in. GS-130 does appear to have some particle deposition that is concentrated mainly on the bottom corners and on the top where the coupon resides in the rack.

Figure 3-101. GS-130 submerged, pre-test (left) and post-test (right).

Figure 3-102. GS-132 submerged, pre-test (left) and post-test (right).

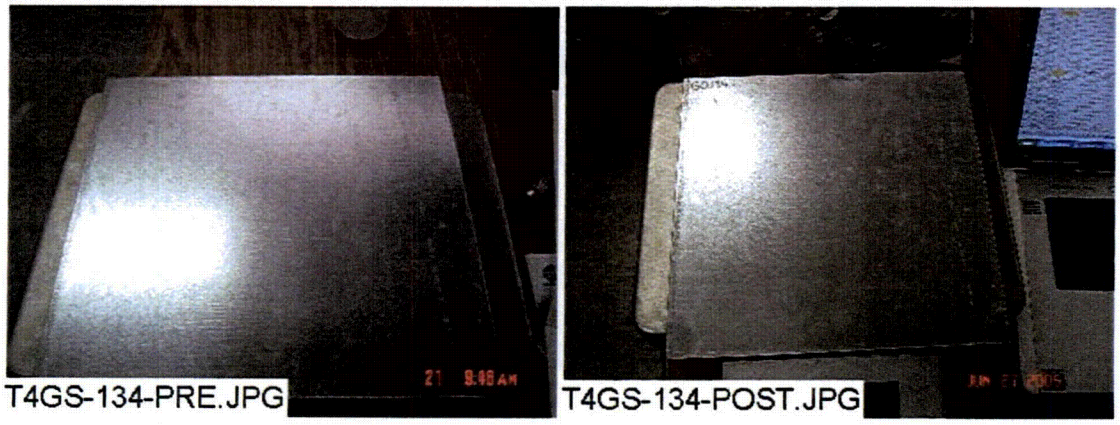

Figure 3-103. GS-134 submerged, pre-test (left) and post-test (right).

Figures 3-104 and 3-105 present the pre- and post-test pictures of two submerged inorganic zinc (IOZ) coated steel coupons. Both submerged IOZ coated steel coupons have similar, light particle depositions. There is a small accumulation of a white precipitate that originates mostly from the points of contact with the racks. However on IOZ-233, the particles seem to be distributed over the majority of the surface of the

coupon. This coupon was the westernmost IOZ coupon in the rack in relation to the others.

Figure 3-104. IOZ-233 submerged, pre-test (left) and post-test (right).

Figure 3-105. IOZ-234 submerged, pre-test (left) and post-test (right).

Figures 3-106 and 3-107 present the pre- and post-test pictures of two submerged copper coupons. The copper coupons were mainly unchanged. Like the other coupons, there is a very light concentration of particulate deposits in the areas where the coupons contact the rack.

Figure 3-106. Cu-548 submerged, pre-test (left) and post-test (right).

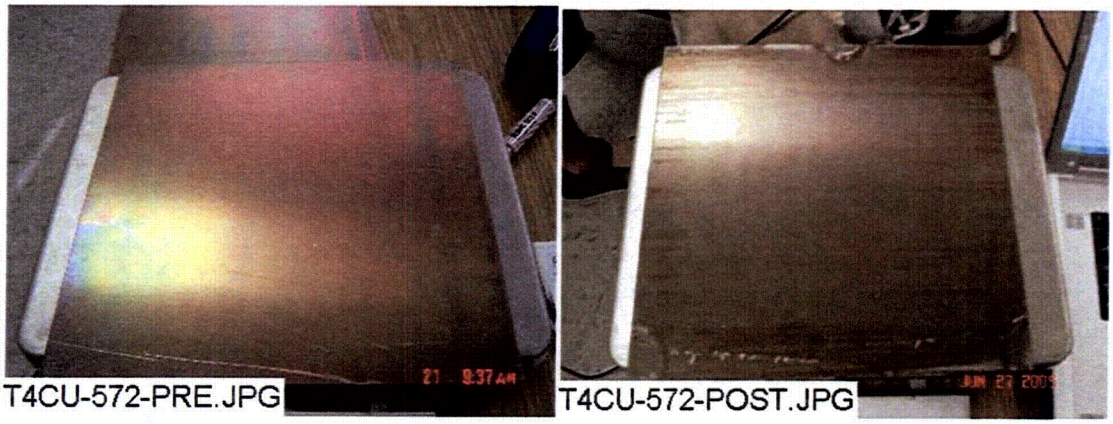

Figure 3-107. Cu-572 submerged, pre-test (left) and post-test (right).

Figure 3-108 presents the pre- and post-test pictures of the submerged carbon steel coupon. Other than some discoloration, there was no change. There was a small amount of rust on the bottom corners.

Figure 3-108. US-17 submerged, pre-test (left) and post-test (right).

Figure 3-109 presents the pre- and post-test pictures of the submerged concrete coupon. The post-test concrete coupon exhibits a brownish color.

Figure 3-109. Conc-004 submerged, pre-test (left) and post-test (right).

Table 3-2 presents the pre- and post-test weight data for each representative submerged coupon.

Table 3-2. Weight Data for Submerged Coupons

Type	Coupon No.	Pre-Test Wt. (g)	Post-Test Wt. (g)	Net Gain/Loss
Al	237	392.1	391.9	-0.2
Al	238	393.1	393.3	0.2
Al	239	392.8	392.8	0.0
GS	130	1042.9	1042.9	0.0
GS	132	1062.1	1062.3	0.2
GS	134	1028.5	1029.0	0.5
IOZ	233	1610.9	1612.6	1.7
IOZ	234	1635.7	1637.9	2.2
CU	548	1300.7	1300.9	0.2
CU	572	1316.7	1316.9	0.2
US	17	1017.4	1017.6	0.2
Conc	04	7950.7	8190.3	239.6

The aluminum coupons average weight differential was zero. This supports the observation that there was little particle deposition. The galvanized steel coupons gained an average of 0.23 g, and the coated steel coupons gained an average of 2.0 g. Both representative copper coupons gained 0.2 g, and the carbon steel coupon also gained 0.2 g. The concrete coupon gained 239.6 g, a gain of 3% of its original weight. The concrete coupon was weighed after sitting in an air environment for one week.

3.4.1.2. Unsubmerged Coupons

Figures 3-110 and 3-111 show the pre- and post-test pictures of two unsubmerged aluminum coupons. Each unsubmerged aluminum coupon accumulated a white particle deposition along with some areas of a brownish color. This coating caused the surface of the aluminum coupons to become coarse and rough. The photo of Al-229 shows that most of the surface is coated with the particle deposition, however, in the upper right hand corner the surface is relatively smooth with a color change observable. This is likely caused by uneven spray on the coupons. Even though the four spray nozzles were set to spray uniformly across their spray radius, the spray was not a perfect mist. There were some non-uniform areas, and the positions of the six coupon racks also interfered with the sprays. Al-003 was loaded in Rack 2 (bottom tier, southernmost), and Al-229 was loaded in Rack 7 (upper tier, northernmost).

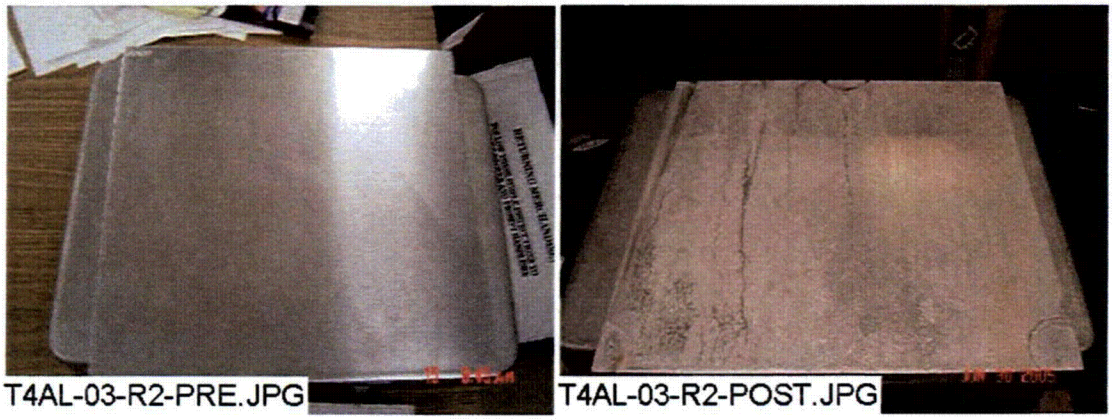

Figure 3-110. Al-003 unsubmerged, pre-test (left) and post-test (right).

Figure 3-111. Al-229 unsubmerged, pre-test (left) and post-test (right).

Figures 3-112 and 3-113 show the pre- and post-test pictures of two unsubmerged galvanized steel coupons. There was some white deposition on the surface of these coupons although it was in small amounts. The post-test coupons were relatively clean,

with little change. GS-33 was mounted in Rack 3 (bottom tier, middle rack), and GS-91 was mounted in Rack 6 (upper tier, middle rack).

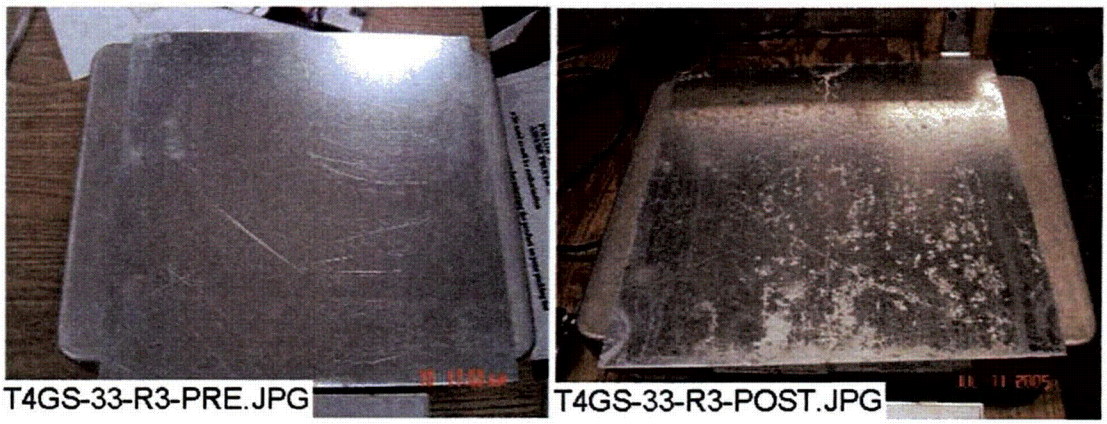

Figure 3-112. GS-33 unsubmerged, pre-test (left) and post-test (right).

Figure 3-113. GS-91 unsubmerged, pre-test (left) and post-test (right).

Figures 3-114 and 3-115 present the pre- and post-test pictures of two unsubmerged copper coupons. All of the copper coupons had vertical water marks that were caused by water flowing downward on the coupon surface during the spray portion of the test. The copper coupons did not appear to accumulate any particle deposition. Cu-536 was mounted in Rack 2 (bottom tier, southernmost), and Cu-584 was mounted in Rack 7 (upper tier, northernmost).

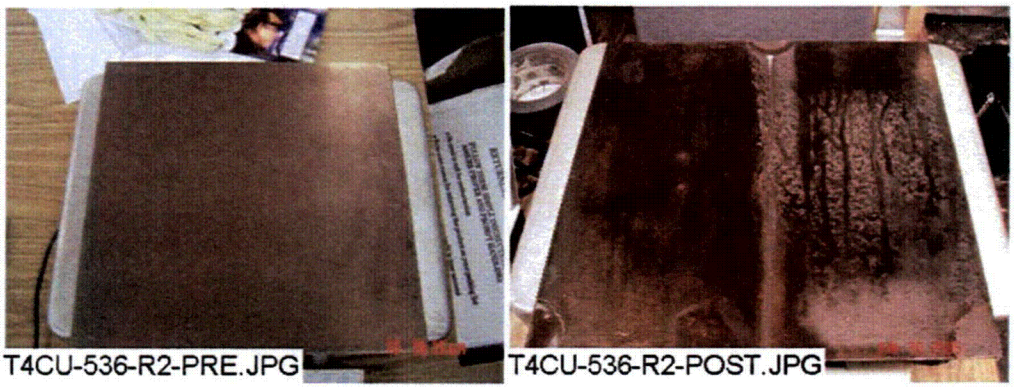

Figure 3-114. Cu-536 unsubmerged, pre-test (left) and post-test (right).

Figure 3-115. Cu-584 unsubmerged, pre-test (left) and post-test (right).

Figures 3-116 and 3-117 present the pre- and post-test pictures of two unsubmerged inorganic zinc coated steel coupons. IOZ-263 was mounted in Rack 4 (bottom tier, northernmost) and IOZ-275 was mounted in Rack 5 (upper tier, northernmost).

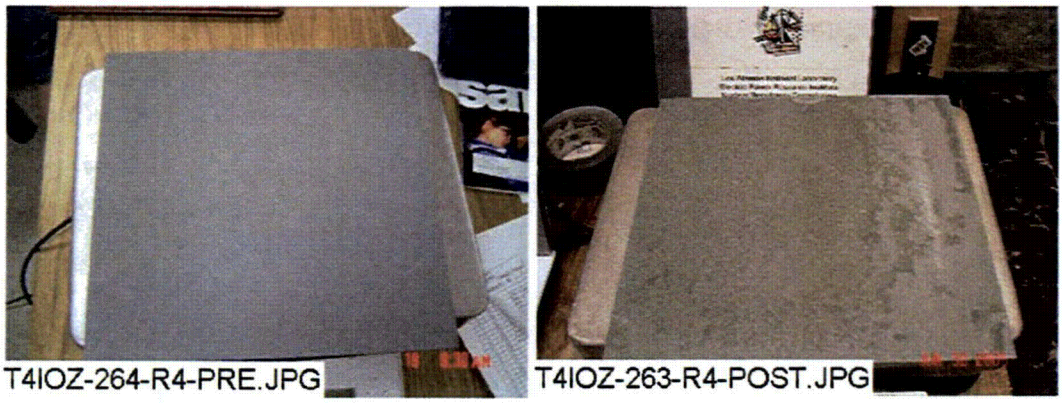

Figure 3-116. IOZ-263 unsubmerged, pre-test (left) and post-test (left).

Figure 3-117. IOZ-275 unsubmerged, pre-test (left) and post-test (right).

Figure 3-118 presents the pre- and post-test pictures of one unsubmerged carbon steel coupon. US-16 was mounted in Rack 6 (upper tier, middle rack).

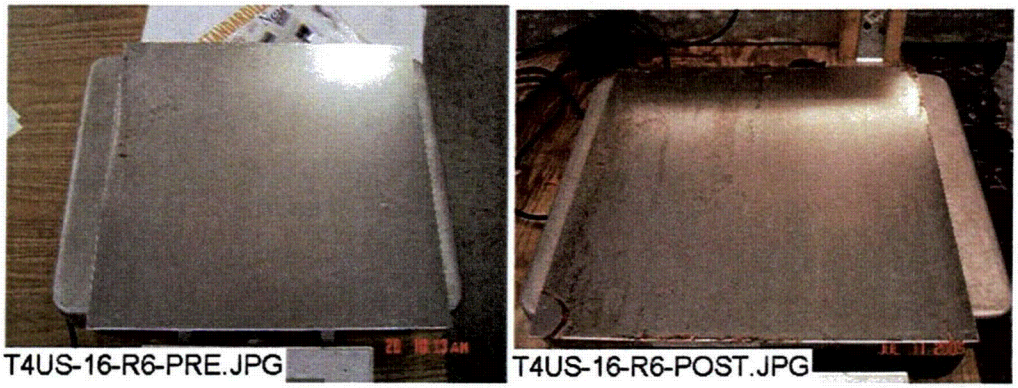

Figure 3-118. US-16 unsubmerged, pre-test (left) and post-test (right).

Table 3-3 presents the pre- and post-test weight data for each representative unsubmerged coupon.

Table 3-3. Weight Data for Unsubmerged Coupons

Type	Coupon No.	Pre-Test Wt. (g)	Post-Test Wt. (g)	Net Gain/Loss
Al	003	391.2	391.7	0.5
Al	229	392.8	394.5	1.7
GS	33	1046.6	1046.6	0.0
GS	91	1030.8	1030.6	-0.2
IOZ	263	1662.0	1662.7	0.7
IOZ	275	1655.0	1657.0	2.0
CU	536	1319.2	1319.3	0.1
CU	584	1334.2	1333.7	-0.5
US	16	1024.1	1023.7	-0.4

The aluminum coupons gained an average of 1.1 g, and the galvanized steel coupons lost an average of 0.1 g. The coated steel coupons average weight gain was 1.4 g, and the copper coupons average weight difference was –0.2 g. The carbon steel coupon lost 0.4 g.

Table 3-4 displays the mean weight gain/loss summary in grams for all of the submerged coupons. Table 3-5 displays the mean weight gain/loss summary in grams for all of the unsubmerged coupons by rack.

Table 3-4. Mean Gain/Loss Data for All Submerged Coupons (g)

Coupon Type	Mean Gain - Loss (g)
AL	0.0
GS	0.3
CU	0.2
IOZ	2.3
US	0.2
Concrete	239.6

Table 3-5. Mean Gain/Loss Data for All Unsubmerged Coupons (g)

Mean Gain-Loss Per Coupon Type (g)					
Rack No.	AL	GS	CU	IOZ	US
2	-0.3	0.8	-0.4	0.8	n/a
3	0.2	1.1	0.2	0.3	n/a
4	-0.4	0.9	-0.2	0.7	-0.8
5	0.1	2.0	<0.1	1.9	n/a
6	-0.5	0.7	-0.4	0.9	-0.4
7	-0.3	0.9	-0.3	1.7	n/a
Overall	0.6	0.2	0.3	1.1	-0.4

3.4.2. SEM Analyses

3.4.2.1. Submerged Coupons

During the ICET tests, trace metal cations may be released from the submerged metal coupon surfaces due to corrosion effects. Subsequently, the released metal cations may complex with the anions from the solution through electrostatic interactions with anions such as OH^-, SiO_3^{2-}, and CO_3^{2-}. More complicated, the complexed anions may attract other cations from the solution, such as Ca^{2+}, Mg^{2+}, Al^{3+}, Cu^{2+}, Zn^{2+}, and H^+. As a result, corrosion products (deposits) are formed and may continuously grow on the metal coupon surfaces. The thickness of the deposits were observed to be in the range of millimeters. The adherence between the metal coupons and the deposits is through chemical bonds, which are much stronger than van der Waals forces. Due to the vertical

orientation of the metal coupons in the tank (with a small horizontal cross-sectional area), the deposits on the metal coupon surface are likely of chemical origin, rather than being the result of particles settling on the surface.

According to SEM/EDS results, the dominant corrosion products on the submerged Al coupons are likely aluminum hydroxide with other substances containing Si, Ca, O, and C. For submerged Cu coupons, the possible corrosion products include CuO, $Cu_2(CO_3)(OH)_2$, and substances containing Ca, Si, Al, and O. For the submerged galvanized steel coupons, the possible corrosion products are oxides, hydroxides, silicate, and carbonate compounds of Zn, Ca, and Al. For the submerged steel coupon, the possible corrosion products include oxide, hydroxide, silicate, and carbonate compounds of Fe and Ca and compounds composed of Fe, Si, Ca, O, and Al.

3.4.2.2. Unsubmerged Coupons

The unsubmerged coupons were affected by the testing solution only during the 4-hour spray phase on the first day of the test and, following that, were affected by water vapor throughout the test.

According to SEM/EDS results, the dominant corrosion products on the unsubmerged Al coupons are likely aluminum hydroxide and/or aluminum oxide, and other corrosion products containing Si, Ca, O, and C. For unsubmerged Cu, the corrosion products on the coupon surface are likely CuO. The corrosion products were composed of C, O, Ca, Si, and Cl on the unsubmerged galvanized steel coupon surface. For the unsubmerged steel coupon, the likely corrosion products are Fe_2O_3, $Fe(OH)_3$, and $Fe_2(CO_3)_3$.

Appendix F contains the SEM data for the coupons.

3.5. Sedimentation

Sediment was collected from the tank bottom after the test solution was drained. It consisted of a particulate sediment that covered the entire tank bottom. Figure 3-119 shows some of this sediment. In addition, Figure 3-120 shows the tank bottom with the sediment, after the samples were removed. Figure 3-121 shows the top of the drain screen with the drain collar surrounded by sediment, and Figure 3-122 shows the drain screen and drain collar after removal from the tank. Figure 3-123 shows the birdcage sitting on top of a basket of cal-sil after the tank was drained. The cal-sil baskets sat on top of the sediment, and thus, the birdcage was not in direct contact with the sediment.

The SEM/EDS and XRD/XRF analyses provided information on the morphology and composition of Test #4 sediment. EDS results show that more than 84% of the sediment was composed of Si, Ca, and O. Consistently, XRF result shows that Si, Ca, and O are the major elements in the composition of the sediment, plus small amounts of Na, Al, Fe, and Mg.

Based on XRD results, the sediment sample contained crystalline substances of tobermorite ($Ca_{2.25}(Si_3O_{7.5}(OH)_{1.5})(H_2O)$) and $Ca_4(Si_6O_{15}(OH)_2)(H_2O)_5$) as well as calcite ($CaCO_3$), which are the same as unused raw or unused baked cal-sil samples. Considering the collective evidence from the EDS, XRF, and XRD analyses, it is likely that the sediment was composed of a significant amount of cal-sil debris, including both raw and baked cal-sil. It should be noted that other deposits such as fiberglass debris and corrosion products may also contribute to the sediments and can not be ruled out.

Figures 3-124 through 3-129 and Table 3-6 provide ESEM/EDS and XRD/XRF analysis results. The complete Day-30 sediment analyses are given in Appendix G.

Figure 3-119. Sediment removed from the tank.

Figure 3-120. Sediment on the tank bottom.

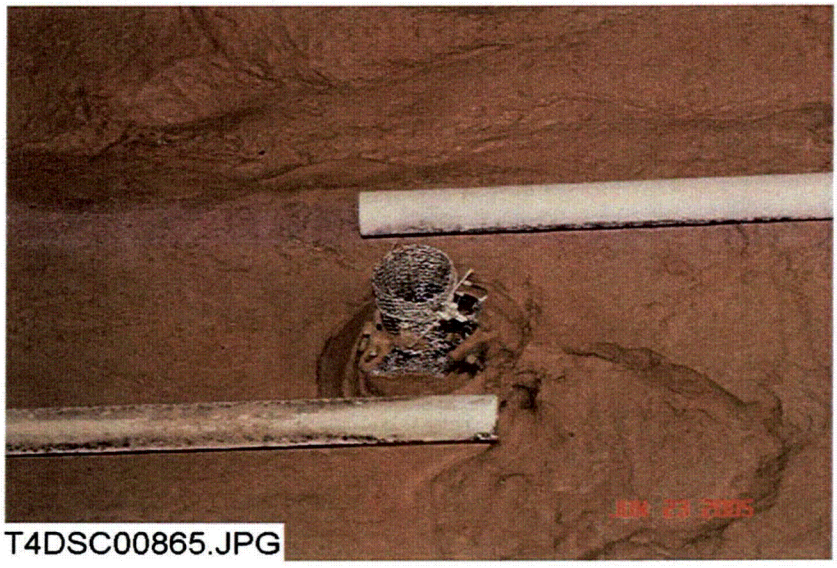

Figure 3-121. Drain collar surrounded by sediment on the tank bottom.

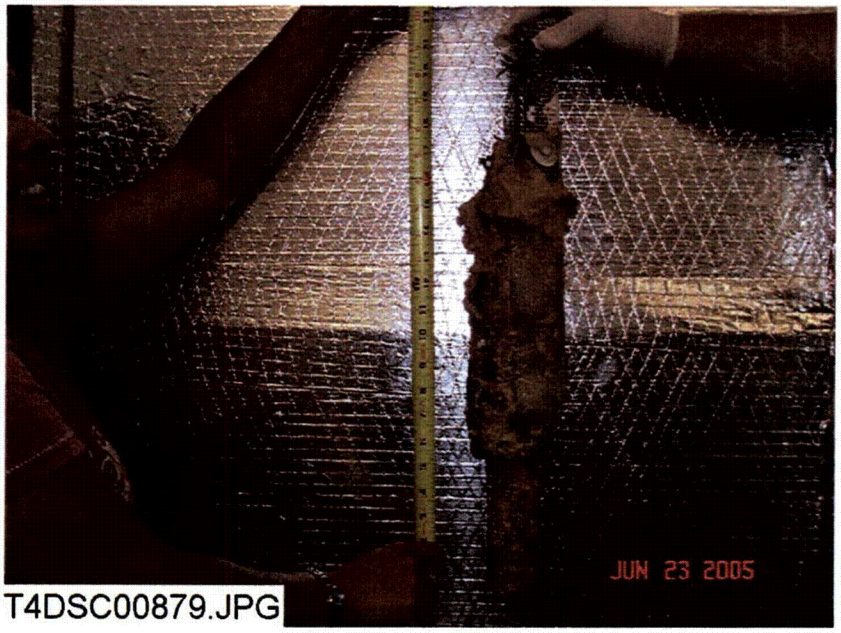

Figure 3-122. Drain collar and drain screen removed from the tank.

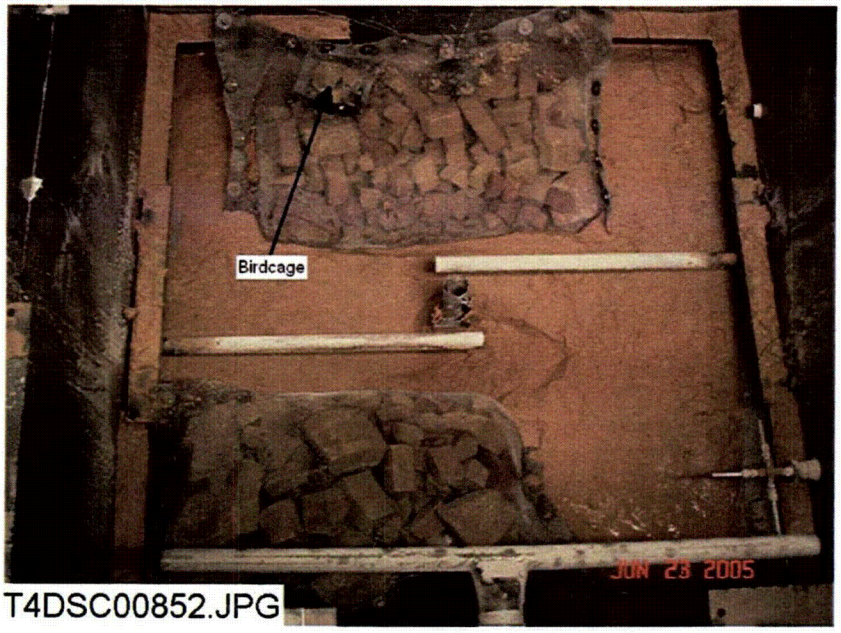

Figure 3-123. Birdcage and cal-sil baskets after the tank was drained.

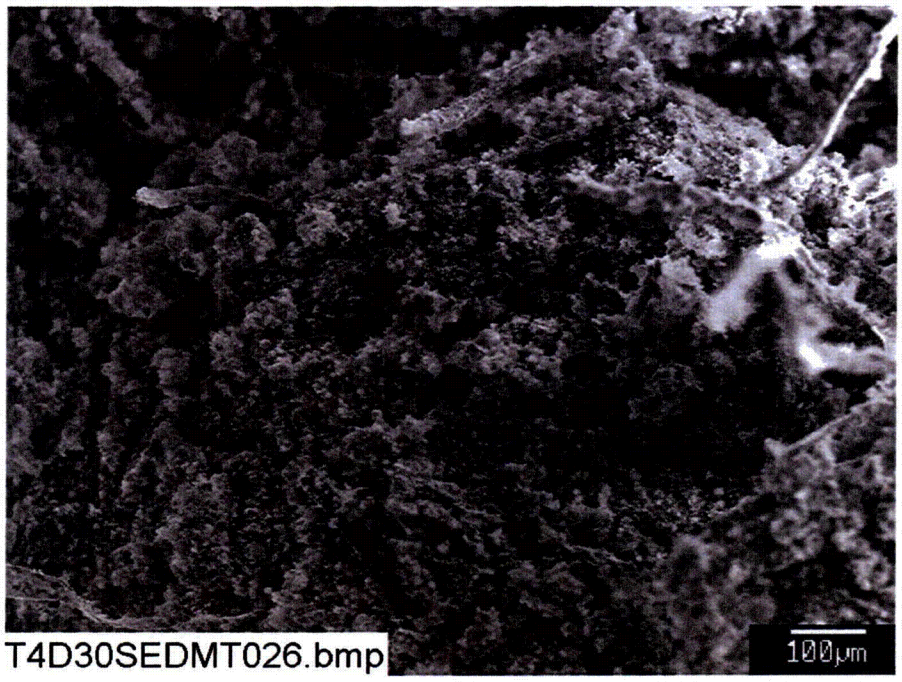

Figure 3-124. SEM image magnified 100 times for a Test #4, Day-30 sediment sample at the bottom of the tank. (T4D30SEDMT026.bmp)

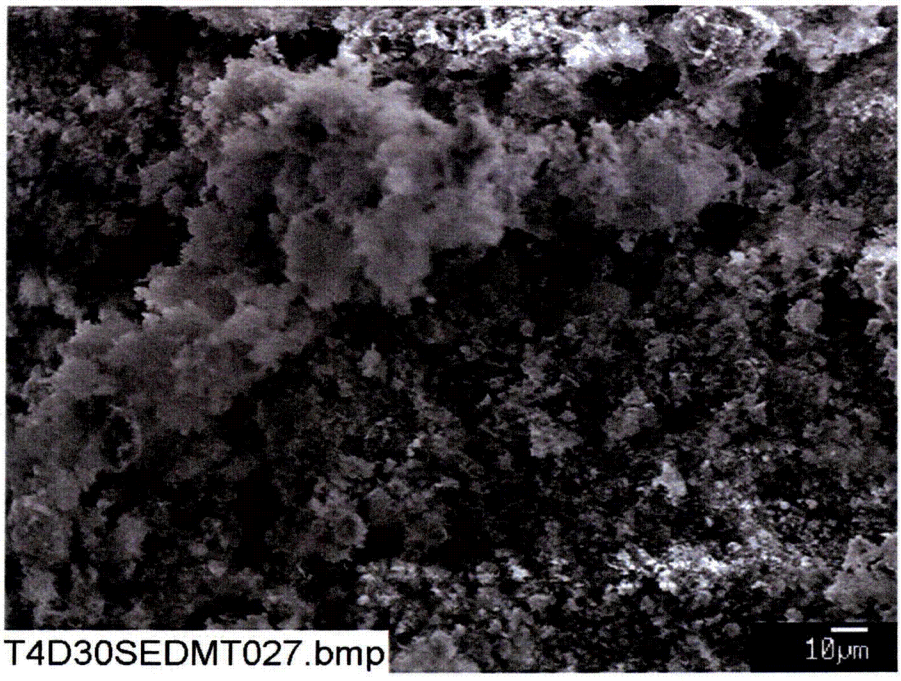

Figure 3-125. SEM image magnified 500 times for a Test #4, Day-30 sediment sample at the bottom of the tank. (T4D30SEDMT027.bmp)

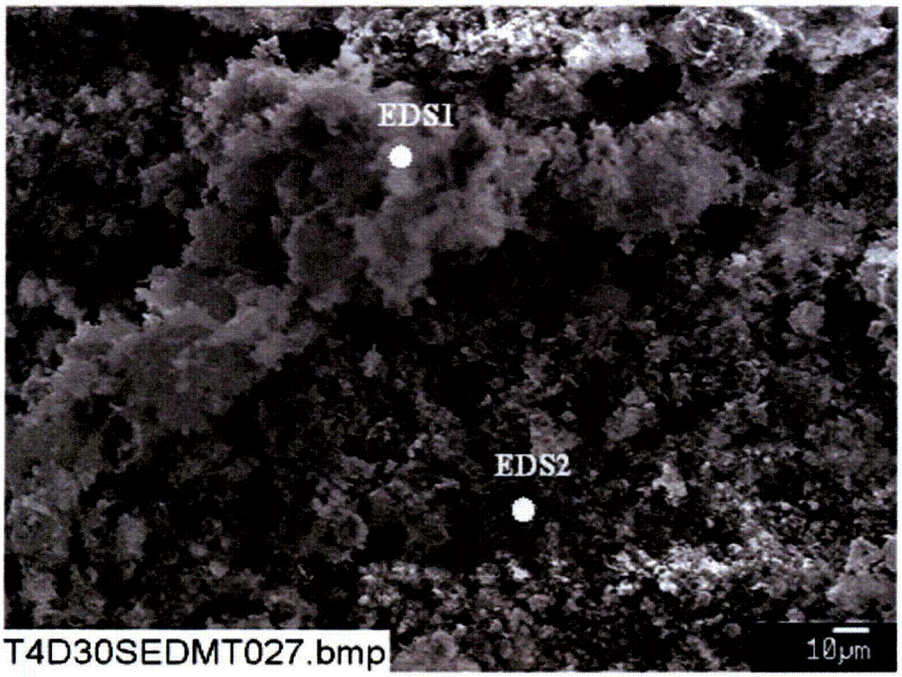

Figure 3-126. Annotated SEM image magnified 500 times for a Test #4, Day-30 sediment sample at the bottom of the tank. (T4D30SEDMT027.bmp)

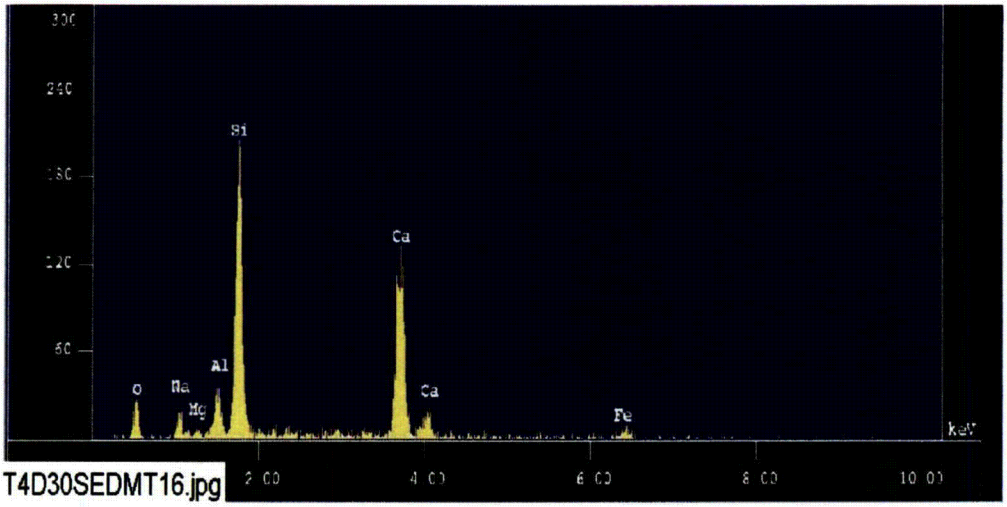

Figure 3-127. EDS counting spectrum for the white snow like deposits (EDS1) shown in Figure 3-126. (T4D30SEDMT16.jpg)

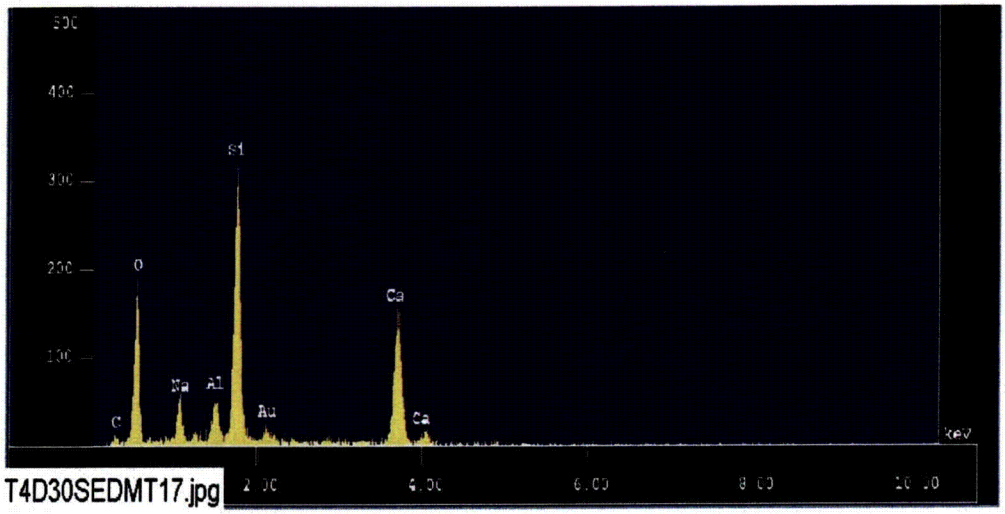

Figure 3-128. EDS counting spectrum for the dark deposits (EDS2) shown in Figure 3-126. (T4D30SEDMT17.jpg)

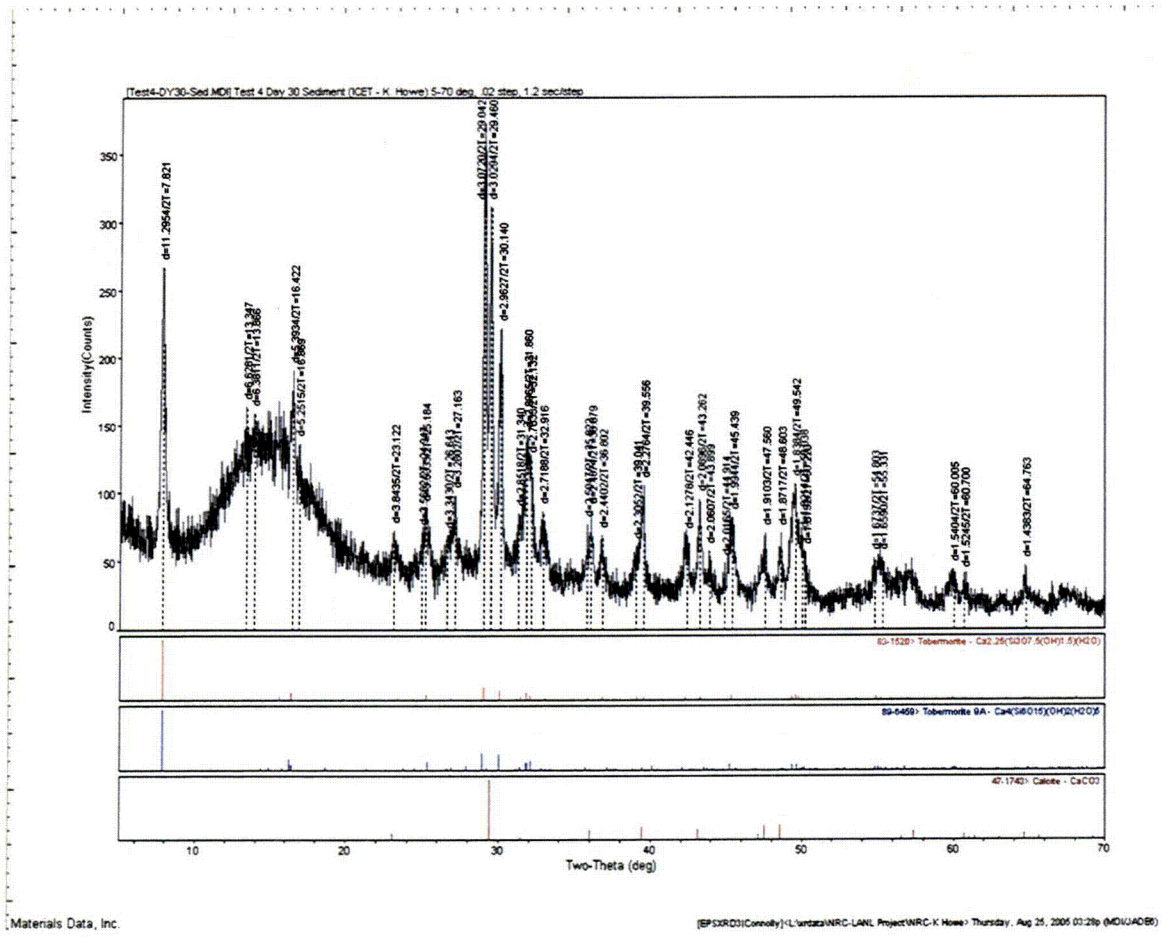

Figure 3-129. XRD result of the possible matching crystalline substances in Test #4, Day-30 sediment.

Table 3-6. Dry Mass Composition of Test #4, Day-30 Sediment by XRF Analysis

First row is chemical component; second row is mass composition (%).

SiO_2	TiO_2	Al_2O_3	Fe_2O_3	FeO	MnO	MgO	CaO	Na_2O	K_2O	$H_20(-)$	$H_2O(+)CO_2$	P_2O_5	Total
34.20	0.18	4.78	2.18	0.00	0.06	0.66	28.58	5.05	0.24	1.25	23.55	0.15	100.88

3.6. Precipitates

Test #4 was markedly different from Test #1 in that no precipitate was found in the test solution, even after it cooled to room temperature. Based on a series of bench-top controlled experiments, the white precipitate observed in Test #1 contained a significant amount of aluminum. The aluminum concentration of the Test #1 solution was as high as 350 mg/L. However, the aluminum in the Test #4 solution occurred only in trace amounts for 2 days and then was below its detection limit.

3.7. Deposition Products

The deposition of debris/corrosion products in the tank after it was drained was observed on the submerged objects in the tank. These corrosion/deposition products, which looked like a fine powder, were collected for analysis. Those collected were from the submerged CPVC coupon rack. SEM/ EDS results indicated that these fine powders were mainly composed of O, Ca, Si, Na, Al, and C. The high content of Ca and Si suggests that the powders were likely from cal-sil and fiberglass debris.

Figure 3-130. SEM image magnified 1000 times for a Test #4, Day-30 fine powder on the submerged rack. (T4D30RackPowder030.bmp)

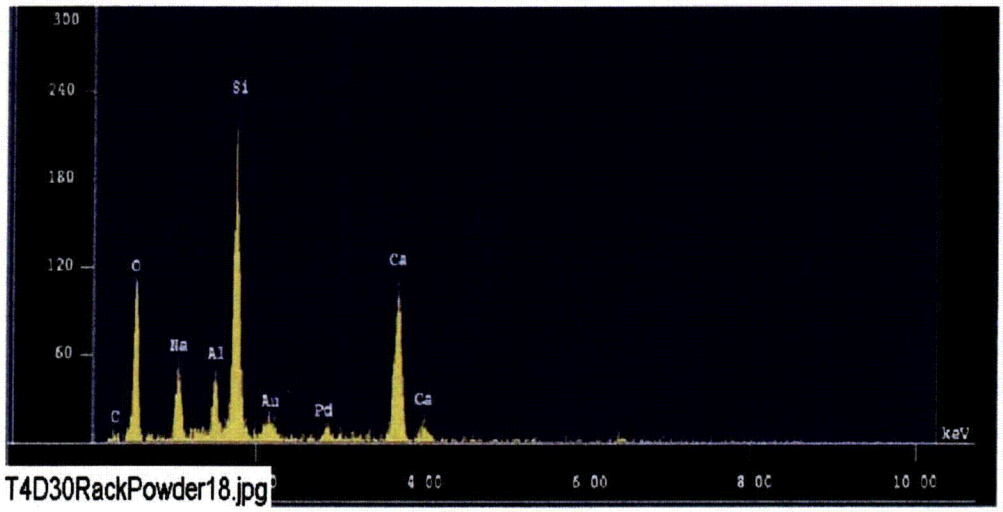

Figure 3-131. EDS counting spectrum for the particles (whole image) shown in Figure 3-130. (T4D30Rackpowder18.jpg)

3.8. Gel Analysis

In ICET Test #3, one significant phenomenon was the presence of white gel-like precipitates in the test solution, especially during and after the injection of TSP on the first day of the test. When Test #3 was shut down, deposits of the pinkish-white gel-like precipitates were observed on the top of the birdcage and on other objects on the tank's bottom. Test #4 had cal-sil and fiberglass samples as did Test #3, however, Test #4 used NaOH instead of TSP. No gel-like material was observed in Test #4.

4. SUMMARY OF KEY OBSERVATIONS

ICET Test #4 ran for 30 days, and all conditions were maintained within the accepted flow and temperature ranges, with two exceptions. On Day 11, a power outage occurred which caused a recirculation pump trip. Recirculation flow was re-established 2 hours and 15 minutes later. During that time, the maximum solution temperature rose to 62.4°C, which is 0.4°C above the target maximum. The maximum temperature was above 62.0°C for approximately one hour. The test solution pH varied from 9.5 to 9.8 over the first two days, rose to 9.9 on Day 8, and then stayed between 9.7 and 9.9 for the remainder of the test. The test solution turbidity decreased to less than 3 NTU after 24 hours. The turbidity continued to decrease and averaged 0.5 NTU over the last three weeks of the test.

Samples of the solution were taken daily. The chemical elements present were calcium, silica, and sodium. Aluminum was present for only the first 24 hours and then only at trace amounts. Strain-rate viscosity measurements indicated that the solution remained Newtonian throughout the test. No precipitates were observed in the solution, even after it had cooled to room temperature.

The submerged metal coupons were relatively unchanged, with light deposits and color changes observed. The IOZ-coated steel coupons had an average weight gain of 2.3 g, and the other metal coupons weight gains were less than 1 g. According to SEM/EDS results, the dominant corrosion products on the submerged Al coupons are likely aluminum hydroxide with other substances containing Si, Ca, O, and C. The other submerged coupons were covered with oxides, hydroxides, and other unidentified compounds. The unsubmerged coupons exhibited some vertical streaking and color changes. The IOZ-coated steel coupons had an average weight gain of 1.1 g, and the other metal coupons weight gains were less than 1 g.

Deposits on the fiberglass samples increased over time, and the deposits appeared to be chemically originated for the samples not lying on the tank bottom. These deposits covered individual fiberglass strands and in some cases formed webs between strands. The deposits did not significantly increase with time in the test solution. It is likely that these deposits were caused by chemical precipitation, since they appear to be soluble. Particulate deposits were evident on samples that were sitting on the tank bottom

In general, particulate deposits were found only on the exterior of the fiberglass. This result suggests that almost all of the particulate deposits were physically retained or attached on the fiberglass exterior. The amount of particulate deposits increases from Day-15 low- and high-flow to the Day-30 high-flow samples. EDS results show that these particulate deposits contain significant amounts of Si and Ca, suggesting they were from cal-sil debris.

Sediment on the tank bottom was prevalent, accumulating to depths of over 8 in. The sediment contained crystalline substances and calcite, making it primarily cal-sil, although some fugitive fiberglass was also present.

REFERENCES

1. "Test Plan: Characterization of Chemical and Corrosion Effects Potentially Occurring Inside a PWR Containment Following a LOCA, Rev. 12c," March 30, 2005.

2. J. Dallman, J. Garcia, B. Letellier, and K. Howe, "Integrated Chemical Effects Tests: Data Compilation for Test 1," LA-UR-05-0124, July 2005.

3. "Pre-Test Operations, Test #4," ICET-PI-015, Rev. 0, May 23, 2005.

4. "Test Operations, Test #4 (cal-sil and fiberglass, and NaOH at pH 10)," ICET-PI-016, Rev. 0, May 23, 2005.

5. "Post-Test Operations, Test #3," ICET-PI-008, Rev. 3, May 2, 2005.

PREFACE TO APPENDICES

Ten separate appendices were developed to capture more of the images and information obtained for Test #4. Several appendices are further divided into subappendices to better segregate the information according to the time point in the test when the samples were extracted from the test apparatus, the location of the samples in the tank, the type of samples being evaluated, and the type of examinations performed. With the exception of Appendix J, each appendix represents a separate session of laboratory work that can be traced to a batch of samples; these samples were typically processed in chronological order. Appendix J provides the detailed project instructions that were used to initiate Test #4, conduct routine operations during the test, and terminate the test with sample recovery and cleaning procedures.

Section 2.4.1.1 of this report reviewed the nomenclature adopted for reporting ICET results. This nomenclature is used in the caption labels for most of the figures presented in the appendices.

As noted in Section 2.4.1.1, the data presented in the appendices are largely qualitative in nature, consisting primarily of SEM and TEM micrographs and EDS spectra. The SEM data are further subdivided into environmental (or low-vacuum) SEM of hydrated samples and microprobe SEM of fully desiccated samples. Microprobe images can be generated using secondary electrons, which are sensitive to attenuation, to reveal fine structural details in a sample or backscatter electrons from the primary beam. Backscatter images indicate in shades of grey with high contrast the relative atomic number of materials across a sample. White or "bright" regions contain high-Z elements; dark regions contain lower-Z elements by comparison.

Transcriptions of the laboratory logbooks are provided for each appendix to document commonalities that existed among the samples at the time of analysis. Logbook information was developed for most, but not all, of the images presented in the appendices. Interpretation and understanding of the images and their accompanying EDS spectra can be improved by referring frequently to the logbook sample descriptions and sequences.

Typically, a relatively large quantity of a test sample was delivered for SEM or TEM analysis, and then several small subsamples of each item were examined. Note that each subsample was assigned a sequential reference number during the laboratory session. These reference numbers have been cited in the figure captions whenever possible to preserve the connection between the micrographs and the notebook descriptions. Electronic filenames have also been stamped on the images to permit retrieval of the original data files, which are archived elsewhere. Individual data sets for a given sample item have been collated into a typical sequence of (1) visual image, (2) EDS spectra, and (3) semiquantitative mass composition.

Semiquantitative mass compositions are also presented for many of the EDS spectra. These results are obtained from a commercial algorithm that decomposes the spectra into

the separate contributions of each element. Composition estimates should be interpreted with the caveats stated in Section 2.4.1.1 fully in mind.

Appendix titles are listed below for reference.

Appendix A. ESEM/EDS Data for Test #4, Day-5 Fiberglass in Low-Flow Zone

Appendix B. ESEM Day-15 Fiberglass
- B1. ESEM/EDS Data for Test #4, Day-15 Fiberglass in Low-Flow Zones
- B2. ESEM/EDS Data for Test #4, Day-15 Fiberglass in High-Flow Zones

Appendix C. ESEM Day-30 Fiberglass
- C1. ESEM/EDS Data for Test #4, Day-30 Fiberglass in Low-Flow Zones
- C2. ESEM/EDS Data for Test #4, Day-30 Fiberglass Inserted in Nylon Mesh in a Low-Flow Zone
- C3. ESEM Data for Test #4, Day-30 Low-Flow Fiberglass Samples in a Big Envelope
- C4. ESEM/EDS Data for Test #4, Day-30 Fiberglass in High-Flow Zones
- C5. ESEM/EDS Data for Test #4, Day-30 Fiberglass Inserted in Front of Header in a High-Flow Zone
- C6. ESEM/EDS Data for Test #4, Day-30 Drain Collar Fiberglass
- C7. ESEM/EDS Data for Test #4, Day-30 Birdcage Fiberglass

Appendix D. ESEM/EDS Data for Test #4, Day-30 Low-Flow Cal-Sil Samples

Appendix E. ESEM and SEM/EDS Data for Test #4, Day-30 Deposition Products

Appendix F. SEM Day-30 Coupons
- F1. SEM/EDS Data for Test #4, Day-30 Aluminum Coupons
- F2. SEM/EDS Data for Test #4, Day-30 Copper Coupons
- F3. SEM/EDS Data for Test #4, Day-30 Galvanized Steel Coupons
- F4. SEM/EDS Data for Test #4, Day-30 Steel Coupons

Appendix G. SEM/EDS Data for Test #4, Day-30 Sediment

Appendix H. TEM Data for Test #4 Solution Samples

Appendix I. UV Absorbance Spectrum—Day-30 Solution Samples

Appendix J. ICET Test #4: Pre-Test, Test, and Post-Test Project Instructions